Discovery of 1-{(3*R*,4*R*)-3-[({5-chloro-2-[(1-methyl-1*H*-pyrazol-4-yl)amino]-7*H*-pyrrolo[2,3-*d*]pyrimidin-4-yl}oxy)methyl]-4-methoxypyrrolidin-1-yl}prop-2-en-1-one (PF-06459988), A Potent, WT Sparing, Irreversible Inhibitor of T790M-Containing EGFR Mutants

Hengmiao Cheng,*[†] Sajiv K. Nair,*[†] Brion W. Murray,*[†] Chau Almaden,[†] Simon Bailey,[†] Sangita Baxi,[†] Doug Behenna,[†] Sujin Cho-Schultz,[†] Deepak Dalvie,[†] Dac M. Dinh,[†] Martin P. Edwards,[†] Jun Li Feng,[†] Rose Ann Ferre,[†] Ketan S. Gajiwala,[†] Michelle D. Hemkens,[†] Amy Jackson-Fisher,[†] Mehran Jalaie,[†] Ted O. Johnson,[†] Robert S. Kania,[†] Susan Kephart,[†] Jennifer Lafontaine,[†] Beth Lunney,[†] Kevin K.-C. Liu,[†] Zhengyu Liu,[†] Jean Matthews,[†] Asako Nagata,[†] Sherry Niessen,[†] Martha A. Ornelas,[†] Suvi T. M. Orr,[†] Mason Pairish,[†] Simon Planken,[†] Shijian Ren,[≠] Daniel Richter,[†] Kevin Ryan,[†] Neal Sach,[†] Hong Shen,[†] Tod Smeal,[†] Jim Solowiej,[†] Scott Sutton,[†] Khanh Tran,[†] Elaine Tseng,[†] William Vernier,[†] Marlena Walls,[†] Shuiwang Wang,[≠] Scott L. Weinrich,[†] Shuibo Xin,[≠] Haiwei Xu,[≠] Min-Jean Yin,[†] Michael Zientek,[†] Ru Zhou,[†] and John C. Kath[†]

[†]La Jolla Laboratories, Pfizer Worldwide Research and Development, 10770 Science Center Drive, San Diego, California 92121, United States

[≠]Wuxi AppTec, 288 Fute Zhong Road, Waigaoqiao Free Trade Zone, Shanghai 200131, China

SUPPORTING INFORMATION

METHODS TO ESTIMATE REVERSIBLE BINDING AFFINITIES OF COVALENT INHIBITORS.

Overview

Incorporating specific chemical reactivity into an inhibitor (covalent inhibition) is an effective mechanism to create kinase-directed drugs with distinct pharmacological properties relative to reversible inhibitors. Covalent inhibitors operate through a two-step process that begins with reversible binding to the intended enzymatic target (described by K_i) followed by covalent bond formation (described by k_{inact}). Reversible interactions are often overlooked and not intentionally optimized, in part, because the methods to evaluate them are not readily available. The precise characterization of all of the covalent inhibitor's rate constants is not necessary in a medicinal chemistry campaign because there is trend analysis (structure-activity relationships) to fortify estimated parameters. A simple, high-capacity method to characterize the reversible component of covalent inhibitor potency was developed to provide a powerful tool to quickly get kinetic data on a large cohort of covalent inhibitors. We now describe this system which can be used in concert with the numerical integration methodology to facilitate biochemical analysis and rational drug design. For covalent inhibitors that do not rely primarily on reactivity to achieve potency, there is sufficient information in the initial enzymatic velocities of the inactivation progress curves to estimate reversible binding affinity of covalent inhibitors. We have developed a method that estimates covalent inhibitor affinity which we term K_i^{est}. The overall inactivation rate (k_{inact}/K_i) is estimated from k_{obs}/I values. Taken together, these kinetic values enable the medicinal chemist a knowledge of the reversible binding affinity and chemical reactivity contributions to overall potency.

Methods

EGFR Kinase Activity Assay

Kinetic analysis of covalent inhibition is facilitated by using highly purified, untagged EGFR proteins which have been previously reported.[1] Covalent inhibitor effects on EGFR activity used an Omnia™ continuous fluorometric assay (Invitrogen, Carlsbad, California) with a Y12 tyrosine phosphoacceptor peptide modified by the chelation-enhanced sulfonamide-oxine fluorophore (cSx), coupled with a cysteine residue (Ac-EEEEYI(cSx)IV-NH_2) (Invitrogen, Carlsbad, CA) and has been previously reported.[1] To simplify the kinetic analysis of covalent inhibitors, experimental conditions are selected to simplify the apparent kinetic mechanism from a reversible bisubstrate, biproduct kinetic mechanism to a single, committed step (low peptide concentration, high ATP concentration).[1]

Estimating Reversible Binding Affinity

All covalent reaction progress curves are nonlinear throughout the entire time course of the assay. However, a crucially important observation that enables this analysis is that the initial slope of the progress curves shown for covalent inhibition of EGFR (more precisely, slope of the tangent to each curve at the initial time $t = 0$) clearly depends on the inhibitor concentration. The changes in the initial slope indicate that, immediately after the enzyme and inhibitor are mixed, a significant fraction of the enzyme instantaneously forms a non-covalent enzyme/inhibitor complex. In other words, the irreversible inhibition of EGFR must proceed in two clearly distinguished mechanistic steps. In the first reversible step (effectively instantaneous on the time scale of these kinetic experiments) we observe the formation of the non-covalent complex. In the second, much slower and irreversible step, we subsequently observe the formation of the

covalent conjugate. Thus we set up assay conditions such that the initial part of the inactivation time-course is dominated by the reversible component of potency (rapid equilibrium condition) while the overall inactivation rate constant (k_{obs}) factors in the chemical reactivity. The initial reaction rates can be analyzed by an algebraic fitting model because the initial enzyme/inhibitor complex is formed instantaneously on the time-scale of the experiment. This "rapid equilibrium" assumption is applicable for all EGFR inhibitors investigated because the empirically determined initial rates vary strongly with the inhibitor concentration and this variation of initial rates follows the equation for competitive inhibition. Covalent inhibitors were measured in duplicate at range of concentrations (5000, 1000, 100, and 50 nM). Background rates were subtracted from the rate data. The slopes of the initial, linear portion of the inactivation progress curves were fit to a linear equation. The linear phase of the time course was typically during the first 200 seconds of each progress curve but more reactive inhibitors (canertinib) deviated from linearity at times less than 200 seconds. The % inhibition values were from the fit of inhibited velocities (v_i) relative to uninhibited velocities (v_o): % inhibition = $(1-(v_i/v_o))*100$. Percent inhibition values were measured in duplicate by determining the initial velocities of uninhibited and inhibited EGFR rates. The % inhibition was converted to estimated K_i values by fitting the data to the equation for competitive inhibition (simple or tight-binding regimes).

Estimating the Overall Inactivation Constant k_{inact}/K_i for Competitive Inhibitors

Covalent inhibitors were evaluated for inhibition of EGFR enzymatic activity at fixed inhibitor concentrations (50, 100, 1000, 5000 nM). Background rates were subtracted from the rate data. The progress curves for irreversible inhibitors were fit to the equation 1 where “A” equals the

fluorescence of fully cleaved peptide substrate (the mathematical function often identified as the "rising exponential with offset"). The k_{obs} is the pseudo-first order rate constant that describes an inactivation time course (product vs time) for the inactivation reaction. Data was analyzed with the non-linear regression analysis program Xlfit4.2 (ID-BS, Guildford, UK).

$$F(t) = \frac{A}{k_{obs}}(1 - e^{-k_{obs}t}) \qquad \text{Eq 1}$$

The k_{obs} values are plotted vs the inhibitor concentration with the slope of the linear relationship being k_{obs}/ [inhibitor] which is known as k_{obs}/I. The k_{obs}/I is the estimated pseudo-second order inhibition constant which measures potency of the inhibitor (k_{obs}/[I] $M^{-1}s^{-1}$) at the concentration of inhibitor tested. The k_{inact}/K_i values were estimated by multiply k_{obs}/I by the ATP saturation factor for a given assay (1 + [ATP]/$K_{m,ATP}$).

BIOCHEMICAL CHARACTERIZATION OF COMPOUND 1 AGAINST EGFR MUTANTS.

Compound **1** (PF-06459988) is a potent inhibitor of EGFR-L858R/T790M, with high affinity (K_i = 13 ± 1 nM), low specific reactivity (k_{inact} of 20 ± 1 ms^{-1}), and high overall potency (k_{inact}/K_i = 1,530,000 ± 114,000 $M^{-1}s^{-1}$). It is also an effective inhibitor of the other major drug-resistant EGFR mutation, EGFR-Del/T790M (K_i = 34 nM, k_{inact}/K_i = 209,000 $M^{-1}s^{-1}$). Towards wild-type EGFR, compound **1** has low affinity (K_i = 1600 ± 100 nM) and low overall potency (k_{inact}/K_i = 4500 ± 200 $M^{-1}s^{-1}$). Compound **1** is a moderately potent inhibitor of EGFR-L858R with relatively weak potency toward EGFR-Del.

Table SI-1. Summary of Enzyme Inhibition Kinetics of Compound 1 Against EGFR Mutants and WT EGFR from k_{obs}/I assay

	L858R/T790M	Del/T790M	L858R	Del	WT
K_i^{est} (nM)	3	34	213	>2100	1600
k_{obs}/I ($M^{-1}S^{-1}$)	42,700	20,400	1410	316	904
k_{inact}/K_i^{est} ($M^{-1}S^{-1}$) (k_{obs}/I*factor)	1,760,000	209,000	17,900	<3000	4520
ATP Saturation Factor	41.2	9.5	5	12.7	9.5

Table SI-2. Global Fit Inactivation Kinetic Parameters for Compound 1 Against L858R/T790M Double Mutant

	K_i (nM)	k_{inact} (s^{-1})	k_{inact}/K_i ($M^{-1}s^{-1}$)
L858R/T790M	13	0.02	1,530,000

EXPERIMENTAL DATA AND SCHEMES.

Starting materials and other reagents were purchased from commercial suppliers and were used without further purification unless otherwise indicated. All reactions were performed under a positive pressure of nitrogen, argon, or with a drying tube, at ambient temperature (unless otherwise stated), in anhydrous solvents, unless otherwise indicated. Analytical thin-layer chromatography was performed on glass-backed Silica Gel 60_F 254 plates (Analtech (0.25mm)) and eluted with the appropriate solvent ratios (v/v).

The reactions were assayed by high performance liquid chromatography (HPLC) or thin-layer chromatography (TLC) and terminated as judged by the consumption of starting material. The TLC plates were visualized by phosphomolybdic acid stain, or iodine stain. Microwave assisted reactions were run in a Biotage Initiator. ^{1}H NMR spectra were recorded on a Bruker instrument operating at 400 MHz unless otherwise indicated. ^{1}H NMR spectra are obtained as DMSO-d_6 or

$CDCl_3$ solutions as indicated (reported in ppm), using chloroform as the reference standard (7.25 ppm) or DMSO-d_6 (2.50 ppm). Other NMR solvents were used as needed. When peak multiplicities are reported, the following abbreviations are used: s = singlet, d = doublet, t = triplet, m = multiplet, br =broadened, dd = doublet of doublets, dt = doublet of triplets. Coupling constants, when given, are reported in hertz. The mass spectra were obtained using liquid chromatography mass spectrometry (LC-MS) on an Agilent instrument using atmospheric pressure chemical ionization (APCI) or electrospray ionization (ESI). High resolution mass measurements were carried out on an Agilent TOF 6200 series with ESI. All test compounds showed > 95% purity as determined by combustion analysis or by high-performance liquid chromatography (HPLC). HPLC conditions were as follows: XBridge C18 column @ 80 °C, 4.6 mm x 150 mm, 5 μm, 5%-95% MeOH/H_2O buffered with 0.2% formic acid/0.4% ammonium formate, 3 min run, flow rate 1.2 mL/min, UV detection (λ = 254, 224 nm). Combustion analyses were performed by Atlantic Microlab, Inc. (Norcross, Georgia).

General Procedures for the Synthesis of 14-21

Step 1: To a solution 2,4,5-trichloro-7H-pyrrolo[2,3-d]pyrimidine (**43**) (1 equiv) and an appropriate alcohol in 1,4-dioxane (0.1 M) in a round bottom flask was added potassium *tert*-pentoxide (4 equiv, 25 % w/w in toluene). The resulting reaction solution was stirred at ambient temperature for 0.5-16 h and reaction completion was monitored by LCMS.

Step 2: To the resulting reaction solution was added the amine (1-1.5 equiv) and *t*-BuXPhos palladacycle (1.1 g, 1.67 mmol, 0.04 -0.05 equiv). The reaction mixture was stirred and heated (thermal conditions: 80- 90 °C for 1 h or under microwave conditions at 140 °C for 30-45 min). The reaction mixture was then filtered through Celite and the filtrate was concentrated and the

corresponding N-Boc amines were either taken on to the next step with no further purification or purified via flash chromatography.

Step 3: To a solution of the *N*-Boc amine (1 equiv) in DCM (60 mL) at 0 °C was added TFA (8 equiv) and the resulting solution was stirred at ambient temperature for 2.5 h. The reaction mixture was concentrated and Et_2O was added to precipitate the corresponding TFA salt as a crude solid residue which was taken on to the next step with no further purification.

Step 4: A mixture of the crude TFA salt (1 equiv), ethyl acetate and saturated aqueous $NaHCO_3$ was stirred at 0 °C for 10 min. Acryloyl chloride, but-2-enoyl chloride or propionyl chloride (1.1 mol. equiv) was added dropwise and the resulting mixture was stirred at ambient temperature for 30 min. Ethyl acetate was added and the organic layer was separated. The aqueous layer was extracted with ethyl acetate and the combined organic layers were dried over Na_2SO_4 and evaporated to give a solid that was purified by SFC. Note: This step also led to desilylation in cases where relevant alcohols had a TBDMS protecting group.

1-((3*R*,4*R*)-3-(((2-((1-Methyl-1*H*-pyrazol-4-yl)amino)-7*H*-pyrrolo[2,3-*d*]pyrimidin-4-yl)oxy)methyl)-4-(trifluoromethyl)pyrrolidin-1-yl)prop-2-en-1-one (**14**):

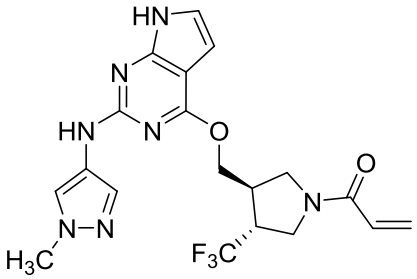

Purified on silica with a gradient of 0-5% ethanol in ethyl acetate to yield the title product (140 mg, 35% yield over 2 steps) LC-MS (APCI) *m*/*z* 436.05 $(M+H)^+$; ^{1}H NMR (400 MHz, $CDCl_3$) δ 7.78 (s, 1 H) 7.53 (s, 1 H) 6.84 (br. s., 1 H) 6.28 - 6.47 (m, 3 H) 5.67 - 5.80 (m, 1 H) 4.61 (dt, *J* = 11.02, 5.45 Hz, 1 H) 4.42 - 4.52 (m, 1 H) 3.91 - 4.06 (m, 2 H) 3.90 (s, 3 H) 3.76 - 3.84 (m, 1 H) 3.63 - 3.72 (m, 1 H) 3.05 - 3.16 (m, 1 H) 2.91 - 3.03 (m, 1 H).

1-{(3*R*)-3-[({5-chloro-2-[(1-methyl-1*H*-pyrazol-4-yl)amino]-7*H*-pyrrolo[2,3-*d*]pyrimidin-4-yl}oxy)methyl]pyrrolidin-1-yl}prop-2-en-1-one (15)

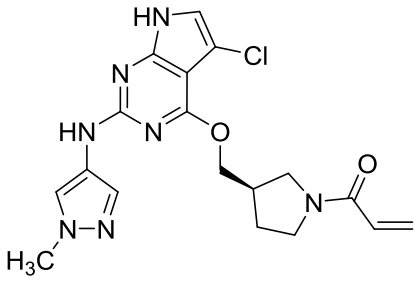

Purified by preparative HPLC (Ac-CHROM, 0.1% TFA, 0-100% ACN in 3 min, 2.25 ml/min) to yield the title compound (106 mg, 47% yield). LC-MS (APCI) *m*/*z* 402.00 $(M+H)^+$; ^{1}H NMR (400 MHz, DMSO-d_6) δ 11.48 (br. s., 1H), 9.03 (s, 1H), 7.85 (s, 1H), 7.52 (s, 1H), 7.04 (s, 1H), 6.58 (ddd, *J* = 3.02, 10.32, 16.87 Hz, 1H), 6.13 (ddd, *J* = 0.76, 2.39, 16.74 Hz, 1H), 5.58 - 5.82 (m, 1H), 4.45 (dq, *J* = 6.80, 10.58 Hz, 2H), 3.71 - 3.88 (m, 4H), 3.55 - 3.70 (m, 2H), 3.34 - 3.53 (m, 1H), 2.63 - 2.90 (m, 1H), 2.01 - 2.24 (m, 1H), 1.71 - 1.97 (m, 1H).

1-((3*R*,4*R*)-3-(((5-Chloro-2-((1-methyl-1*H*-pyrazol-4-yl)amino)-7*H*-pyrrolo[2,3-*d*]pyrimidin-4-yl)oxy)methyl)-4-(trifluoromethyl)pyrrolidin-1-yl)prop-2-en-1-one (**16**):

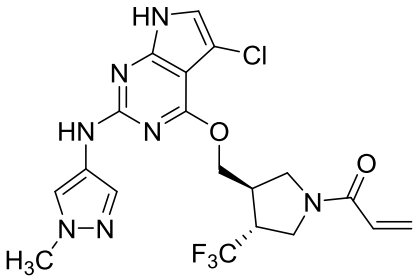

Purified with Waters CSH C18. 3.5um. 10mM NH_4OAc, 2.25 mL/min, 140 bar to yield the title compound (133 mg, 54% yield); LC-MS (APCI) *m*/*z* 470.10 $(M+H)^+$; ^1H NMR (400 MHz, DMSO-d_6) δ 11.44 (br. s., 1 H) 9.07 (s, 1 H) 7.85 (s, 1 H) 7.51 (s, 1 H) 7.05 (s, 1 H) 6.48 - 6.73 (m, 1 H) 6.08 - 6.21 (m, 1 H) 5.61 - 5.76 (m, 1 H) 4.39 - 4.64 (m, 2 H) 3.73 - 4.14 (m, 6 H) 3.59 - 3.72 (m, 1 H) 3.50 (dd, *J* = 12.63, 5.56 Hz, 1 H) 2.89 - 3.12 (m, 1 H).

1-((3*R*,4*R*)-3-(((5-Chloro-2-((1-methyl-1*H*-pyrazol-4-yl)amino)-7*H*-pyrrolo[2,3-*d*]pyrimidin-4-yl)oxy)methyl)-4-fluoropyrrolidin-1-yl)prop-2-en-1-one (**17**):

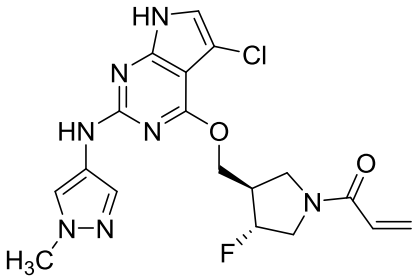

trans-racemic product purified by chiral SFC Chiralcel OJ-H 4.6 x 250 mm column, 25% EtOH, 140 bar, 3.0 mL/min) to give the title compound (102 mg, 34% yield): LC-MS (APCI) *m*/*z* 419.9 $(M+H)^+$ with Cl isotope pattern; ^1H NMR (400 MHz, DMSO-d_6) δ 11.50 (br. s., 1 H) 9.08 (s, 1 H) 7.85 (s, 1 H) 7.51 (s, 1 H) 6.98 - 7.08 (m, 1 H) 6.59 (ddd, *J* = 18.13, 16.84, 10.27 Hz, 1 H) 6.15 (dd, *J* = 16.81, 2.38 Hz, 1 H) 5.64 - 5.73 (m, 1 H) 5.20 - 5.54 (m, 1 H) 4.37 - 4.57 (m, 2 H)

3.82 - 4.17 (m, 2 H) 3.79 (s, 3 H) 3.56 - 3.77 (m, 2 H) 2.83 - 3.17 (m, 1 H); ^{19}F NMR (376 MHz, DMSO-d_6) δ -173.68 (br. s., 1 F).

1-((3*R*,4*R*)-3-(((5-Chloro-2-((1-methyl-1*H*-pyrazol-4-yl)amino)-7*H*-pyrrolo[2,3-*d*]pyrimidin-4-yl)oxy)methyl)-4-hydroxypyrrolidin-1-yl)prop-2-en-1-one (**18**):

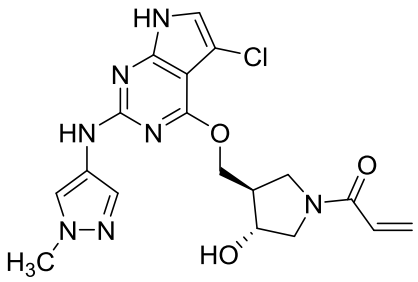

Purified by HPLC/10 mM ammonium acetate to yield the title compound (23 mg, 27% yield): LC-MS (APCI) *m*/*z* 418.10 $(M+H)^+$; ^{1}H NMR (400 MHz, DMSO-d_6) δ 9.07 (s, 1 H) 7.86 (br. s., 1 H) 7.50 (s, 1 H) 7.04 (d, *J* = 1.11 Hz, 1 H) 6.56 (td, *J* = 17.21, 10.37 Hz, 1 H) 6.12 (dd, *J* = 16.72, 2.35 Hz, 1 H) 5.66 (dt, *J* = 10.30, 2.73 Hz, 1 H) 4.50 (br. s., 1 H) 4.39 (br. s., 1 H) 4.28 (d, *J* = 4.70 Hz, 1 H) 3.85 - 3.97 (m, 1 H) 3.79 (s, 3 H) 3.64 - 3.71 (m, 1 H) 3.59 (dd, *J* = 10.64, 5.39 Hz, 1 H) 3.21 - 3.29 (m, 2 H) 2.55 - 2.69 (m, 1 H).

1-((3*R*,4*R*)-3-(((5-Chloro-2-((1-methyl-1*H*-pyrazol-4-yl)amino)-7*H*-pyrrolo[2,3-*d*]pyrimidin-4-yl)oxy)methyl)-4-(hydroxymethyl)pyrrolidin-1-yl)prop-2-en-1-one (**19**):

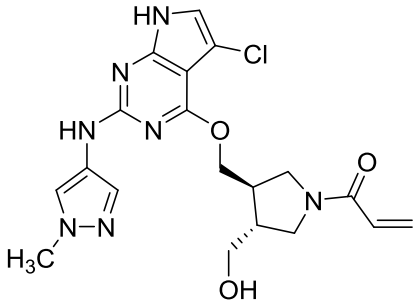

Purified by chiral SFC (Chiralcel OD-H 4.6x250 mm column, 40% EtOH, 60% CO_2, 140 bar, 3.0 mL/min) to yield the title compound (52 mg, 22% yield): LC-MS (APCI) *m*/*z* 432.90 $(M+H)^+$; ^{1}H NMR (400 MHz, DMSO-d_6) δ 11.31 - 11.50 (m, 1 H) 8.98 (s, 1 H) 7.79 (s, 1 H) 7.44 (s, 1 H) 6.97 (d, *J*=2.27 Hz, 1 H) 6.43 - 6.63 (m, 1 H) 5.98 - 6.16 (m, 1 H) 5.47 - 5.69 (m, 1 H) 4.65 - 4.82 (m, 1 H) 4.45 - 4.59 (m, 1 H) 4.24 - 4.39 (m, 1 H) 3.73 (s, 5 H) 3.44 - 3.54 (m, 1 H) 3.31 - 3.43 (m, 1 H) 3.12 - 3.22 (m, 1 H) 2.47 - 2.64 (m, 1 H) 2.12 - 2.34 (m, 1 H).

1-((3*R*,4*R*)-3-(((5-Chloro-2-((1-methyl-1*H*-pyrazol-4-yl)amino)-7*H*-pyrrolo[2,3-*d*]pyrimidin-4-yl)oxy)methyl)-4-(methoxymethyl)pyrrolidin-1-yl)prop-2-en-1-one (**20**):

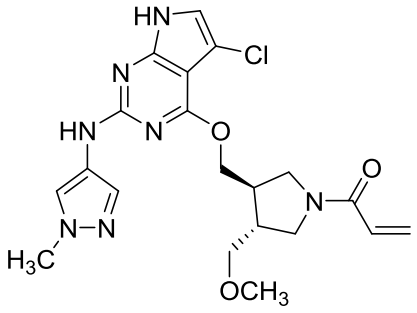

Purified by chiral SFC (Chiralpak AD-H 4.6x250 mm column, 50% EtOH, 50% CO_2, 140 bar, 3.0 mL/min) to yield the title compound (67 mg, 29% yield): LC-MS (APCI) *m*/*z* 444.25 $(M+H)^+$; ^{1}H NMR (400 MHz, DMSO-d_6) δ 11.50 (br. s., 1 H) 9.06 (s, 1 H) 7.85 (s, 1 H) 7.52 (s, 1 H) 7.05 (d, *J* = 1.76 Hz, 1 H) 6.42 - 6.74 (m, 1 H) 6.12 (dt, *J* = 16.81, 1.79 Hz, 1 H) 5.49 - 5.76 (m, 1 H) 4.51 - 4.60 (m, 1 H) 4.47 (d, *J* = 5.29 Hz, 1 H) 3.88 (d, *J* = 7.55 Hz, 1 H) 3.80-3.82 (m, 4 H) 3.48 - 3.60 (m, 1 H) 3.35 - 3.43 (m, 1 H) 3.28 - 3.34 (m, 4 H) 3.17 (d, *J* = 5.04 Hz, 1 H) 2.56 - 2.65 (m, 1 H) 2.35 - 2.46 (m, 1 H).

1-((3*S*,4*S*)-3-(((5-Chloro-2-((1-methyl-1*H*-pyrazol-4-yl)amino)-7*H*-pyrrolo[2,3-*d*]pyrimidin-4-yl)oxy)methyl)-4-methoxypyrrolidin-1-yl)prop-2-en-1-one (**21**):

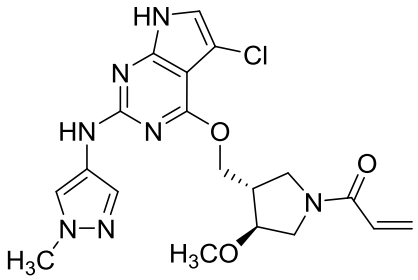

Purified by chiral SFC (Whelk-O1 (R, R) 4.6x250 mm 10/100 column, 30% EtOH, 70% CO_2, 140 bar, 3.0 mL/min) to yield the title compound (94 mg, 30% yield): LC-MS (APCI) *m/z* 432.90 $(M+H)^+$; ^{1}H NMR (400 MHz, DMSO-d_6) δ 11.16 (br. s., 1 H) 8.61 (s, 1 H) 7.72 (s, 1 H) 7.44 (d, *J* = 0.76 Hz, 1 H) 6.87 (s, 1 H) 6.46 (dd, *J* = 16.87, 10.58 Hz, 1 H) 6.03 (dd, *J* = 16.87, 2.52 Hz, 1 H) 5.55 (dd, *J* = 10.45, 2.39 Hz, 1 H) 4.25 - 4.50 (m, 2 H) 3.90 (m, *J* = 16.90 Hz, 2 H) 3.66 - 3.74 (m, 3 H) 3.29 - 3.58 (m, 3 H) 3.23 (s, 3 H) 2.55 - 2.83 (m, 1 H).

Purified Intermediates after Step 2

***tert*-Butyl-(*R*)-3-(((5-chloro-2-((1-methyl-1*H*-pyrazol-4-yl)amino)-7*H*-pyrrolo[2,3-*d*]pyrimidin-4-yl)oxy)methyl)pyrrolidine-1-carboxylate (15a)**:

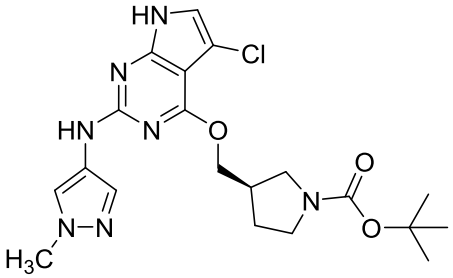

Purified via flash column chromatography with EtOAc to give the title compound as a brown colored oil (257 mg, 64% yield): LC-MS (ESI) *m/z* 448.20 $(M+H)^+$; ^{1}H NMR (400 MHz, DMSO-d_6) δ 11.23 (br. s., 1 H) 8.69 (s, 1 H) 7.82 (d, *J* = 0.50 Hz, 1 H) 7.54 (d, *J* = 0.76 Hz, 1 H) 6.96 (d, *J* = 2.27 Hz, 1 H) 4.29 - 4.68 (m, 2 H) 3.81 (s, 3H) 3.52 (dd, *J* = 10.83, 7.55 Hz, 1 H)

3.37 - 3.46 (m, 1 H) 3.29 (dt, *J* = 10.58, 7.55 Hz, 1 H) 3.21 (dd, *J* = 10.95, 6.92 Hz, 1 H) 2.71 (dt, *J* = 14.23, 7.24 Hz, 1 H) 2.01 - 2.16 (m, 1 H) 1.80 (dq, *J* = 12.37, 7.88 Hz, 1 H) 1.42 (s, 9 H).

***tert*-Butyl-(3*R*,4*R*)-3-(((5-chloro-2-((1-methyl-1*H*-pyrazol-4-yl)amino)-7*H*-pyrrolo[2,3-*d*]pyrimidin-4-yl)oxy)methyl)-4-(trifluoromethyl)pyrrolidine-1-carboxylate** (**16a**):

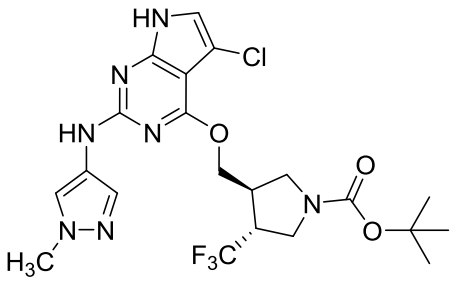

Purified on silica with a gradient of 0-100% ethyl acetate in heptanes to yield the title compound (279.3mg, 44% yield): LC-MS (APCI) *m*/*z* 516.0 $(M+H)^+$; ^{1}H NMR (400 MHz, DMSO-d_6) δ 11.50 (br. s., 1 H) 9.07 (s, 1 H) 7.85 (br. s., 1 H) 7.51 (s, 1 H) 7.05 (d, *J* = 2.27 Hz, 1 H) 4.37 - 4.63 (m, 2 H) 3.79 (s, 3 H) 3.70 - 3.78 (m, 1 H) 3.61 - 3.69 (m, 1 H) 3.44 (dd, *J* = 11.62, 5.31 Hz, 1 H) 3.32 - 3.40 (m, 1 H) 3.22 - 3.30 (m, 1 H) 2.88 - 2.98 (m, 1 H) 1.39 (s, 9 H).

***tert*-Butyl-(3*R*,4*R*)-3-(((5-chloro-2-((1-methyl-1*H*-pyrazol-4-yl)amino)-7*H*-pyrrolo[2,3-*d*]pyrimidin-4-yl)oxy)methyl)-4-fluoropyrrolidine-1-carboxylate** (**17a**):

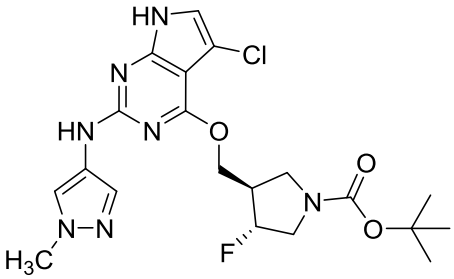

Purified on silica with gradients from 100% heptane to 100% ethyl acetate (Rf 0.4 (UV) in 100% ethyl acetate) to give the title compound (330 mg, 51% yield in 2 steps, >90% purity): LC-MS

(APCI) *m*/*z* 466.1 $(M+H)^+$ with Cl isotope pattern; ^{1}H NMR (400 MHz, DMSO-d_6) δ 11.50 (br. s., 1 H) 9.06 (s, 1 H) 7.85 (s, 1 H) 7.51 (s, 1 H) 7.05 (s, 1 H) 5.16 - 5.45 (m, 1 H) 4.45 (d, *J* = 6.06 Hz, 2 H) 3.80 (s, 4 H) 3.47 - 3.64 (m, 2 H) 3.41 (t, *J* = 11.49 Hz, 1 H) 2.82 - 3.03 (m, 1 H) 1.39 (s, 9 H).

***tert*-Butyl-(3*R*,4*R*)-3-(((5-chloro-2-((1-methyl-1*H*-pyrazol-4-yl)amino)-7*H*-pyrrolo[2,3-*d*]pyrimidin-4-yl)oxy)methyl)-4-hydroxypyrrolidine-1-carboxylate (18a)**:

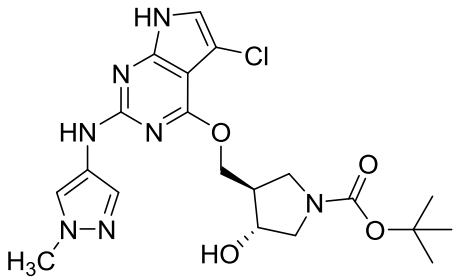

Purified on silica with gradients from 20-50-100% ethyl acetate in heptanes to yield the title compound (123 mg, 57% yield): LC-MS (APCI) *m*/*z* 478.15 $(M+H)^+$; ^{1}H NMR (400 MHz, DMSO-d_6) δ 11.19 (br. s., 1 H) 8.62 (br. s., 1 H) 7.75 (s, 1 H) 7.48 (d, *J* = 0.50 Hz, 1 H) 6.91 (d, *J* = 2.52 Hz, 1 H) 4.32 - 4.47 (m, 3 H) 3.72 - 3.76 (m, 3 H) 3.49 - 3.61 (m, 3 H) 3.09 (d, *J* = 3.78 Hz, 2 H) 1.36 (s, 9 H) 0.78 - 0.82 (m, 9 H) 0.00 (d, *J* = 4.03 Hz, 6 H).

***tert*-Butyl-(3*R*,4*R*)-3-(((tert-butyldimethylsilyl)oxy)methyl)-4-(((5-chloro-2-((1-methyl-1*H*-pyrazol-4-yl)amino)-7*H*-pyrrolo[2,3-*d*]pyrimidin-4-yl)oxy)methyl)pyrrolidine-1-carboxylate (19a)**:

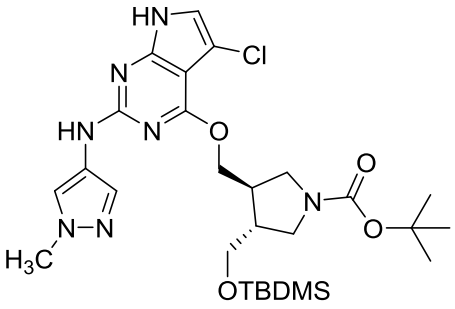

Purified via flash column chromatography with EtOAc to give the title compound as a brown colored oil (338 mg, 86% yield): LC-MS (ESI) *m/z* 592.30 $(M+H)^+$; ^{1}H NMR (400 MHz, DMSO-d_6) δ10.98 - 11.61 (m, 1 H) 8.62 (s, 1 H) 7.78 (s, 1 H) 7.50 (s, 1 H) 6.93 (d, *J* = 2.52 Hz, 1 H) 4.29 - 4.54 (m, 2 H) 3.77 (s, 3 H) 3.72 (d, *J* = 5.29 Hz, 1 H) 3.45 - 3.63 (m, 3 H) 3.10 - 3.27 (m, 2 H) 2.49 - 2.54 (m, 1 H) 2.22 - 2.38 (m, 1 H) 1.38 (s, 9 H) 0.83 (s, 9 H) 0.01 (s, 3 H) 0.00 (s, 3 H).

***tert*-Butyl-(3*R*,4*R*)-3-(((5-chloro-2-((1-methyl-1*H*-pyrazol-4-yl)amino)-7*H*-pyrrolo[2,3-*d*]pyrimidin-4-yl)oxy)methyl)-4-(methoxymethyl)pyrrolidine-1-carboxylate** (**20a**):

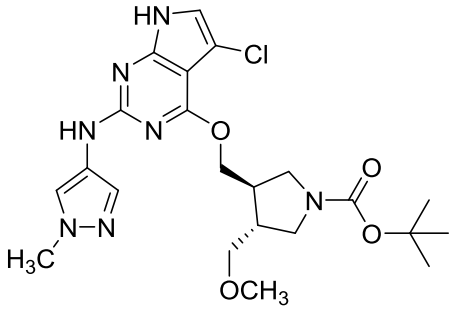

Purified via flash column chromatography with a gradient 0-1% MeOH/EtOAc to give the title compound as a brown colored oil (269 mg, 68% yield): LC-MS (ESI) *m/z* 491.30 $(M+H)^+$; ^{1}H NMR (400 MHz, DMSO-d_6)δ ppm 11.49 (br. s., 1 H) 9.05 (s, 1 H) 7.85 (s, 1 H) 7.52 (s, 1 H) 7.05 (d, *J* = 2.52 Hz, 1 H) 4.48 - 4.60 (m, 1 H) 4.33 - 4.45 (m, 1 H) 3.80 (s, 3 H) 3.45 - 3.59 (m, 2 H) 3.28 - 3.40 (m, 5 H) 2.96 - 3.20 (m, 2 H) 2.31 - 2.48 (m, 2 H) 1.39 (s, 9 H).

***tert*-Butyl-(3*S*,4*S*)-3-(((5-chloro-2-((1-methyl-1*H*-pyrazol-4-yl)amino)-7*H*-pyrrolo[2,3-*d*]pyrimidin-4-yl)oxy)methyl)-4-methoxypyrrolidine-1-carboxylate** (**21a**):

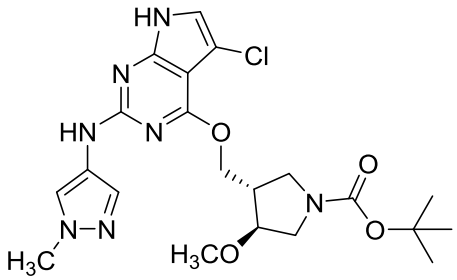

Purified via flash column chromatography with EtOAc to give the title compound as a brown colored oil (368 mg,71% yield): LC-MS (ESI) *m*/*z* 478.20 $(M+H)^+$; ^{1}H NMR (400 MHz, DMSO-d_6) δ 11.25 (br. s., 1H), 8.70 (s, 1H), 7.82 (s, 1H), 7.54 (d, *J* = 0.76 Hz, 1H), 6.97 (s, 1H), 4.30 - 4.64 (m, 2H), 3.88 - 3.99 (m, 1H), 3.81 (s, 3H), 3.63 (dd, *J* = 5.41, 11.71 Hz, 1H), 3.54 (dd, *J* = 7.55, 11.08 Hz, 1H), 3.27 - 3.37 (m, 5H), 2.61 - 2.78 (m, 1H), 1.41 (s, 9H).

Preparation of *N*-(4-((3-chloro-4-fluorophenyl)amino)-7-(prop-2-yn-1-yloxy)quinazolin-6-yl)acrylamide (**22**)**.**

Step 1: Preparation of 6-nitro-7-(prop-2-yn-1-yloxy)quinazolin-4(3H)-one

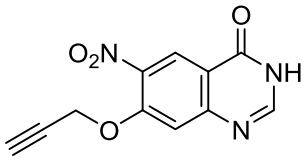

To a solution of prop-2-yn-1-ol (8.7 g, 0.156 mol) in THF (300 mL) was added NaH (6.9 g, 0.172 mol) at 0 °C. After stirring for 1 h at 15 °C, 7-fluoro-6-nitroquinazolin-4(3H)-one (16.3 g, 0.078 mol) was added. The mixture was stirred at 70 °C for 10 h. LC-MS showed the reaction

was complete. The mixture was filtered and the filter cake was dried under reduced pressure to afford title compound (35 g) as a brown solid which was taken to the next step without any further purification.

Step 2: Preparation of 4-chloro-6-nitro-7-(prop-2-yn-1-yloxy)quinazoline

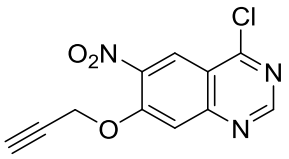

The mixture of 6-nitro-7-(prop-2-yn-1-yloxy)quinazolin-4(3H)-one (3.5 g, 0.014mol) in $POCl_3$ (100 mL) was stirred at 120 °C for 3 h. TLC (petroleum ether: EtOAc = 2:1) showed the reaction was completed. After removal of $POCl_3$, the title compound was obtained as an oil which was taken to the next step without any further purification.

Step 3: Preparation of *N*-(3-chloro-4-fluorophenyl)-6-nitro-7-(prop-2-yn-1-yloxy)quinazolin-4-amine

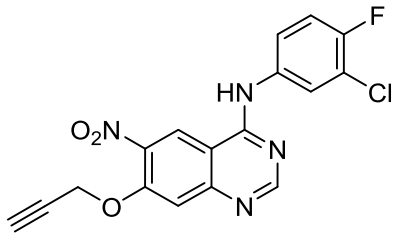

To a solution of 4-chloro-6-nitro-7-(prop-2-yn-1-yloxy)quinazoline (3.7 g, 0.014 mol) and 3-chloro-4-fluoroaniline (3.7 g, 0.025 mol) in 1,4-dioxane (150 mL) was added HCl/MeOH (3.5 mL). The mixture was stirred at 100 °C for 18 h. TLC (petroleum ether: EtOAc = 2:1) showed the reaction was completed. After removal of dioxane, the residue was dissolved in EtOAc /THF

(300 mL, 4:1) and washed with water (200 mL) and saturated $NaHCO_3$ (100 mL). The organic phase was dried over anhydrous Na_2SO_4, filtered and concentrated. The residue was purified by column chromatography eluting with petroleum ether: EtOAc = 2.6:1 to afford title compound as a yellow solid (2.63 g, 51%).

Step 4: Preparation of N^4-(3-chloro-4-fluorophenyl)-7-(prop-2-yn-1-yloxy)quinazoline-4,6-diamine

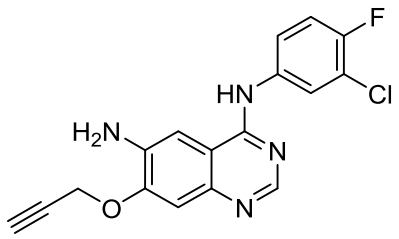

To a solution of *N*-(3-chloro-4-fluorophenyl)-6-nitro-7-(prop-2-yn-1-yloxy)quinazolin-4-amine (6.4 g, 0.014 mol) in H_2O/EtOH (1:10, 220 mL) was added Fe (4.8 g, 0.085 mol) and NH_4Cl (5.4 g, 0.102 mol). The mixture was sonicated while swirling by hand for 2 min, and stirred at 80 °C for 3 h. LC-MS showed the reaction was completed. After filtration, the solution was concentrated. Water (200 mL) was added to the residue and the mixture was stirred at 20 °C for 30 min. The mixture was then filtered and the filter cake was dried under reduced pressure to afford title compound as yellow solid (3.8 g, 65%): LC-MS *m/z* for $C_{17}H_{12}ClFN_4O$ 343.2 $(M+H)^+$; ^1H NMR (400 MHz, DMSO-d_6) δ10.47 (s, 1H), 8.63 (s, 1H), 8.05 (s, 1H), 7.71 (s, 1H), 7.51 (d, 2H), 7.29 (s, 1H), 5.83 (s, 2H), 5.09 (s, 2H), 3.78(s, 2H).

Step 5: Preparation of *N*-(4-((3-chloro-4-fluorophenyl)amino)-7-(prop-2-yn-1-yloxy)quinazolin-6-yl)acrylamide (**22**)

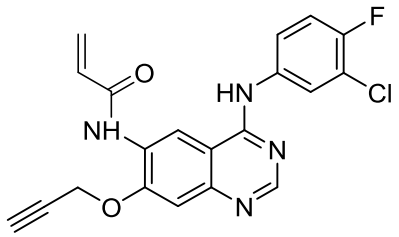

N^4-(3-chloro-4-fluorophenyl)-7-(prop-2-yn-1-yloxy)quinazoline-4,6-diamine (400 mg, 1.16 mmol) was suspended in CH_2Cl_2/THF (1:5, 100 mL). DIPEA (0.6 mL, 3.48 mmol) was added to the suspension and the mixture was stirred for ten minutes. Acryloyl chloride (157.4 mg, 1.74 mmol) was then added dropwise. During this period, the suspension first turned clear and then became cloudy again. After stirring for an hour, LC-MS showed the reaction was complete. The mixture was quenched with water (1 mL) and concentrated. The residue was purified by preparative HPLC to afford title compound as yellow solid (156.5 mg, 34%): LC-MS *m/z* for $C_{20}H_{14}ClFN_4O_2$ 396.9 $[M+H]^+$; ^{1}H NMR (400 MHz, DMSO-d_6) δ 9.83 (d, 2H), 8.92 (s, 1H), 8.55 (s, 1H), 8.12 - 8.14 (m, 1H), 7.79 - 7.82 (m, 1H), 7.41 - 7.44 (m, 2H), 6.71 - 6.77 (m, 1H), 6.32 (d, 1H), 5.82 (d, 1H), 5.11 (s, 2H), 3.72 (s, 1H).

_N_-(3-((7-(hydroxymethyl)-2-((4-(4-methylpiperazin-1-yl)phenyl)amino)-7_H_-pyrrolo[2,3-_d_]pyrimidin-4-yl)oxy)phenyl)acrylamide (32)

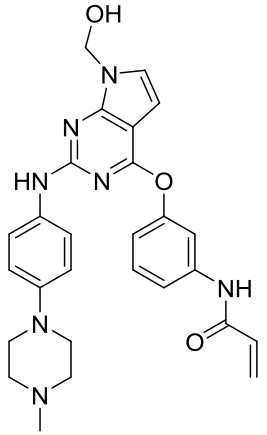

^{1}H NMR (400 MHz, DMSO-d_6) δ 10.24 (s, 1 H) 8.92 (s, 1 H) 7.47 - 7.59 (m, 2 H) 7.26 - 7.43 (m, 3 H) 7.07 (d, *J* = 3.54 Hz, 1 H) 6.82 - 6.94 (m, 1 H) 6.60 (d, *J* = 8.84 Hz, 2 H) 6.30 - 6.42 (m, 1 H) 6.12 - 6.25 (m, 2 H) 5.64 - 5.74 (m, 1 H) 5.38 (s, 2 H) 2.84 - 2.96 (m, 4 H) 2.30 - 2.37 (m, 4 H) 2.12 (s, 3 H).

Synthesis of crystalline HBr salt of amine 46: 5-chloro-4-{[(3R,4R)-4-methoxypyrrolidin-3-yl]methoxy}-*N*-(1-methyl-1*H*-pyrazol-4-yl)-7*H*-pyrrolo[2,3-*d*]pyrimidin-2-amine (HBr salt)

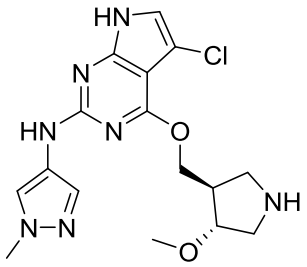

Compound **46** (TFA salt) was suspended in saturated aqueous $NaHCO_3$ (10 mL). Foam formed but there was no solid after a while. The mixture was extracted with 10% isopropanol in DCM (2 x 70 ml), dried over Na_2SO_4 and evaporated to give a residue (115 mg). This residue was dissolved in ethanol (4.5 ml) and HBr (29 uL, 0.26 mmol, 48 wt%) was added. Additional HBr 3 x 29 µL was added sequentially. As the solution became cloudy, it was stirred and heated at 50 ºC (heating block) for 15 min. The mixture was cooled to RT without stirring. After 2 days, white solid was collected by filtration, washed with ethanol (3 mL) and dried (10 mmHg ca. 60 ºC) to give a white solid (104 mg, 38% yield): LC-MS (APCI) *m/z* 377.8 ($M+H^+$); ^{1}H NMR (400MHz, DMSO-d_6) δ 11.53 (br. s., 1H), 9.07 (br. s., 3H), 7.85 (s, 1H), 7.54 (s, 1H), 7.07 (d, *J* = 2.3 Hz, 1H), 6.59 - 5.64 (m, 3H), 4.48 (d, *J* = 6.5 Hz, 2H), 4.16 - 4.05 (m, 1H), 3.81 (s, 3H), 3.59 - 3.47 (m, 1H), 3.45 - 3.34 (m, 2H), 3.32 (s, 3H), 3.14 (qd, *J* = 6.0, 12.1 Hz, 1H), 2.87 (t, *J* =

6.3 Hz, 1H). The structure of **1** was confirmed by small molecule X-ray diffraction of the crystalline HBr salt of the precursor amine **46**.

Synthesis of *tert*-butyl (3*R*,4*R*)-3-(hydroxymethyl)-4-(trifluoromethyl)pyrolidine-1-carboxylate via a Cal B Lipase resolution.

Step 1: Synthesis of ethyl (E)-5,5,5-trifluoropent-2-enoate

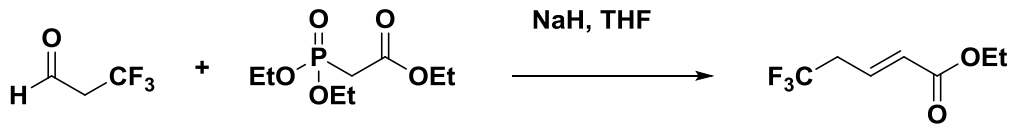

To a stirred suspension of NaH (60% in mineral oil, 2.15 g, 53.5 mmol) in dry THF (50 mL) was added dropwise ethyl(diethoxyphosphoryl)acetate (11 g, 49 mmol) at 0 °C under a N_2 atmosphere. The resulting mixture was stirred at 0 °C for 10 min and cooled to -70 °C. A solution of 3,3,3-trifluoropropanal (5.0 g, 44.5 mmol) in dry THF (50 mL) was added to the mixture at -70 °C. After the addition, the stirred mixture was allowed to warm to -20 °C over 2 h. The reaction mixture was quenched by addition of 5% aqueous NH_4C1(100mL) at 0 °C and extracted with EtOAc (100 mL). The organic layer was washed with brine (300 mL), dried over Na_2SO_4 and concentrated. The residue was purified by flash chromatography (petroleum ether : EtOAc, 100:1) to give the title compound (3.0 g, 37%) as a colorless oil. The ^{1}H NMR matched the literature reported ^{1}H NMR (*Journal of the Chemical Society, Perkin Transactions 1: Organic and Bio-Organic Chemistry (1972-1999)* **1991**, (9), 2147).

Step 2: Synthesis of ethyl 1-benzyl-4-(trifluoromethyl)pyrrolidine-3-carboxylate

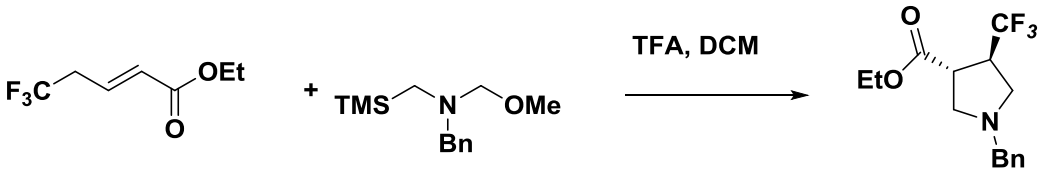

To a stirred solution of ethyl (2*E*)-5,5,5-trifluoropent-2-penoate (3.0 g, 16.5 mmol) and TFA (3.8 g, 33 mmol) in DCM (40 mL) was added dropwise 1-benzyl[(trimethylsilyl)methyl]-amino)methanol (7.8 g, 33 mmol) at 0 °C over a period of 30 min. After the addition, the mixture was heated under reflux overnight. TLC (petroleum ether : EtOAc, 10:1) indicated ethyl (2*E*)-5,5,5-trifluoropent-2-enoate was consumed. The reaction mixture was washed with sat. $NaHCO_3$ (40 mL), brine (40 mL), dried over Na_2SO_4 and concentrated. The residue was purified by flash chromatography (petroleum ether: EtOAc, 100:1 to 10 : 1) to give the title compound (5.1 g, 98% yield) as a yellow oil. LC-MS *m/z* 302.1 $(M+H)^+$; ^1H NMR (400 MHz, CDCl3) δ 7.24 - 7.37 (m, 5 H) 4.19 (q, *J* = 7.22 Hz, 2 H) 3.56 - 3.70 (m, 2 H) 3.29 - 3.47 (m, 1 H) 3.07 - 3.16 (m, 1 H) 2.76 - 2.95 (m, 3 H) 2.71 (dd, *J* = 9.82, 6.04 Hz, 1 H) 1.27 (t, *J* = 7.18 Hz, 3 H).

Step 3: Cal B Lipase Hydrolysis

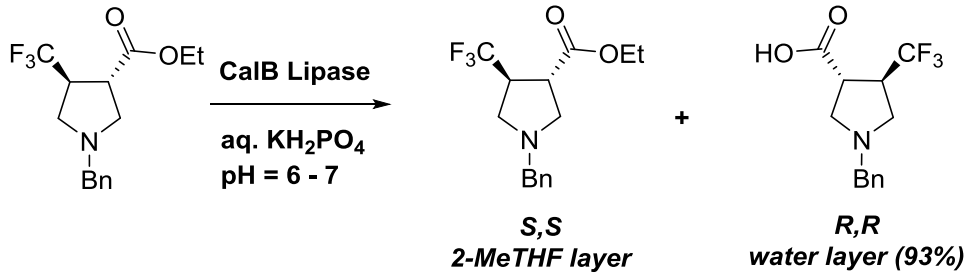

To a 250 mL flask was added ethyl 1-benzyl-4-(trifluoromethyl)pyrrolidine-3-carboxylate (15.5 g, 51.3 mmol) followed by water (56 mL) and 1 M H_3PO_4 (4.0 mL). The reaction mixture was heated to 35 °C and 3.7 mL of Novozymes CAL B Lipase was added. The reaction was held at 35 °C for 15 min. The pH of the reaction was found to be 4 – 5. K_3PO_4 (600 mg) in water (3

mL) was added and stirring was continued for 42 h, while checking the progress by LCMS. After 42 h, a 1:1 ratio of acid to ester was observed by LCMS-TIC area% and the reaction was cooled to room temperature. The reaction was worked up in the following manner: THF (66 mL) and aq. HCl (9 mL of 2.5 N) was added to dissolve most of the material. The mixture was filtered through a pad of Celite® washing with 2-MeTHF (3 x 70 mL). Solid K_3PO_4 (14 g) and water (10 mL) were added until pH = 11 was reached and the ester was extracted with 2-MeTHF (3 x 70 mL). The combined organic layer was dried over Na_2SO_4 and evaporated to afford the crude (*S*,*S*)-ester which was set aside. The aqueous layer (120 mL) was evaporated to dryness. Then, 2-MeTHF (200 mL) was added and the mixture was filtered through Celite® washing with 2-MeTHF to remove most of the inorganic salts. After evaporating off the solvents, 7.4 grams (93%) of a white foam was obtained, as the potassium salt of the acid. The LCMS of this crude material showed ~90% purity. A 300 mg portion of the acid salt was purified by prep-HPLC followed by recrystallization from iPrOH to obtain an analytical sample of the free acid with > 98% ee by chiral SFC. Note: the (S,S)-ester from above was hydrolyzed (LiOH) and used as a standard to ensure the SFC method could separate the two acid enantiomers. LC-MS *m/z* 274 $(M+H)^+$; ^{1}H NMR (400 MHz, MeOH-d_4) δ 7.17 - 7.37 (m, 5 H) 3.64 - 3.71 (m, 1 H) 3.49 - 3.58 (m, 2 H) 3.37 - 3.49 (m, 1 H) 3.00 - 3.09 (m, 1 H), 2.92 - 3.00 (m, 1 H) 2.69 - 2.80 (m, 2 H) 2.65 (t, *J* = 8.06 Hz, 1 H); $[\alpha]_d^{25}$ = +12.3° (c = 1.13, MeOH).

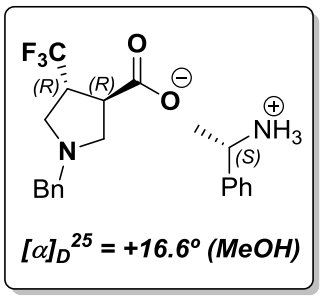

The absolute configuration was determined to be R,R by comparison of the above sample to the optical properties and the x-ray crystal structure reported in *Bioorg & Med Chem Lett* **1998**, 8, 2833 as follows: The analytical sample of acid from above was mixed (1:1 ratio) with (*S*)-alphamethyl benzyl amine in MeOH. Salt crystals formed immediately which were recrystallized from iPrOH. The optical rotation of this salt was $[\alpha]_d^{25}$ = +16.6° (c = 0.5, MeOH) which was opposite and equal to the (*S*,*S*)-salt of (*R*)-α-methyl benzyl amine salt reported (lit. for the *S*,*S*-salt with of (*R*)-alphamethyl benzyl amine $[\alpha]_d^{25}$ = -17.5° (c = 1.0, MeOH).

Step 4: Synthesis of ((3*R*,4*R*)-1-benzyl-4-(trifluoromethyl)pyrrolidin-3-yl)methanol

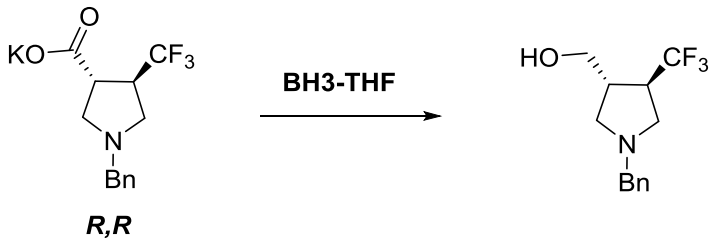

R,R

To a solution of potassium (3*R*,4*R*)-1-benzyl-4-(trifluoromethyl)pyrrolidine-3-carboxylate (10.7 g, 34.4 mmol) in THF (100 mL) at 0 °C under a nitrogen atmosphere was slowly added BH_3-THF (75 mL of 1.0M in THF, 75 mmol). The resulting solution was allowed to warm to ambient temperature and stirred for 2 h. The reaction was cooled to 0 °C and carefully quenched with methanol (25 mL, added very slowly). The volatiles were removed to give a white solid residue and methanol (100 mL) was added for the second time. After stirring for 30 min, the solvents were removed and MeOH (100 mL) was added a 3rd time and the reaction was stirred for 18 h. The volatiles were removed to afford a white residue. This residue was purified via flash chromatography eluting with a gradient of 100% heptane to 100% EtOAc, maintaining 100% EtOAc. Product fractions were combined and evaporated to give a colorless oil (5.9 g, 66% yield over 2 steps). LC-MS *m/z* 260.1 $(M+H)^+$; ^{1}H NMR (400 MHz, $CDCl_3$) δ 7.22 - 7.38 (m, 5

H) 3.76 (dd, *J* = 10.45, 3.40 Hz, 1 H) 3.62 (s, 3 H) 2.98 - 3.19 (m, 2 H) 2.77 - 2.92 (m, 2 H) 2.54 - 2.63 (m, 1 H) 2.46 (dt, *J* = 6.74, 3.05 Hz, 1 H) 2.40 (dd, *J* = 9.57, 7.81 Hz, 1 H); 96% de by chiral SFC.

Step 5: Synthesis of *tert*-butyl (3*R*,4*R*)-3-(hydroxymethyl)-4-(trifluoromethyl)pyrrolidine-1-carboxylate

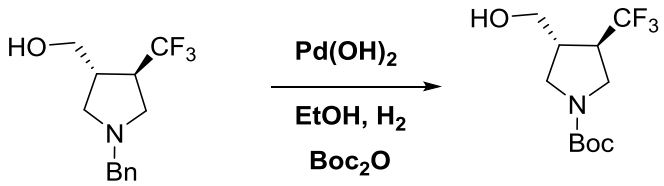

To a solution of [(3*R*,4*R*)-1-benzyl-4-(trifluoromethyl)pyrrolidin-3-yl]methanol (7.84 g, 30 mmol) in ethanol (200 mL) was added Boc anhydride (6.6 g, 30 mmol). The resulting solution was degassed with nitrogen and $Pd(OH)_2$ (20 wt%, wet, 1 g) was added. The reaction was placed under 1 atm of H_2 at ambient temperature with stirring for 20 h. The catalyst was removed and the filtrate was evaporated to give 8.4 g as a colorless oil with 96% de based on chiral SFC analysis. The sample was purified by preparative chiral SFC using a Chiralpak IC 4.6 x 250 mm 5µ column, eluting with 5% MeOH, 140 bar CO_2, 3.0 mL/min. The chiral preparative method yielded 7.2 g (96%) of tert-butyl (3*R*,4*R*)-3-(hydroxymethyl)-4-(trifluoromethyl)pyrrolidine-1-carboxylate. LC-MS *m/z* 170 $(M+H)^+$ – Boc; ^{1}H NMR (400 MHz, $CDCl_3$) δ 3.57 - 3.75 (m, 4 H) 3.22 - 3.58 (m, 2 H) 2.89 (br. s., 1 H) 2.58 (br. s., 1 H) 2.07 - 2.47 (m, 1 H), 1.46 (s, 9 H); $[\alpha]_d^{25}$ = +34.5° (c=2, $CDCl_3$).

Preparation of *tert*-butyl (3*S*,4*S*)-3-(((*tert*-butyldimethylsilyl)oxy)methyl)-4-(hydroxymethyl)pyrrolidine-1-carboxylate

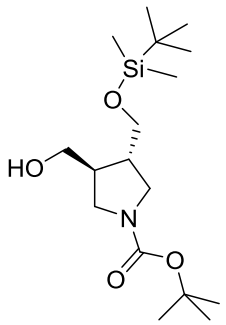

$LiBH_4$ (911 mg, 39.7 mmol) was added to a solution of 1-(*tert*-butyl) 3-ethyl (3*S*,4*S*)-4-(((tert-butyldimethylsilyl)oxy)methyl)pyrrolidine-1,3-dicarboxylate (3.08g, 7.95 mmol) in THF (25 mL). The resulting mixture was heated to reflux for 3 h. The reaction was quenched with water (100 ml) and stirred at room temperature for 1 h. The mixture was extracted with EtOAc (150 mL). The organic layer was washed with brine, dried over Na_2SO_4 and evaporated to give colorless oil. The crude product was purified via flash chromatography eluting with 30% EtOAc in heptane to give the title compound as colorless oil (2.34 g, 86%). ^{1}H NMR (400 MHz, $CDCl_3$) δ 3.69 - 3.81 (m, 1H), 3.58 - 3.67 (m, 2H), 3.50 - 3.54 (m, 2H), 3.37 - 3.46 (m, 1H), 2.88 - 3.07 (m, 2H), 2.19 - 2.20 (m, 2H), 1.46 (s, 9H), 0.92 (s, 9H), 0.10 (s, 6H).

Preparation of *tert*-butyl (3*S*,4*S*)-3-(hydroxymethyl)-4-(methoxymethyl)pyrrolidine-1-carboxylate

Step 1: Synthesis of *tert*-butyl (3*S*,4*S*)-3-(((*tert*-butyldimethylsilyl)oxy)methyl)-4-(methoxymethyl)pyrrolidine-1-carboxylate

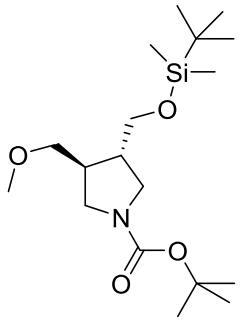

Tetrabutylammonium iodide (0.110 g, 0.28 mmol), 50% aqueous NaOH (20 mL) and dimethyl sulfate (0.325 mL, 3.41 mmol) were added to a solution of *tert*-butyl (3*S*,4*S*)-3-(((tert-butyldimethylsilyl)oxy)methyl)-4-(hydroxymethyl)pyrrolidine-1-carboxylate (0.982 g, 2.84 mmol) in CH_2Cl_2 (20 mL). The reaction was stirred at RT for 18 h. Additional dimethyl sulfate (0.150 mL) was added and the mixture was stirred at RT for 3 h. Aqueous NH_4OH (28%, 30 mL) was added to the reaction mixture and stirred at RT for 1h. The mixture was diluted with H_2O (20 mL) and extracted with CH_2Cl_2 (2x30 mL). The combined organic layers were dried over $MgSO_4$ and concentrated. The residue was purified via flash chromatography eluting with 10% EtOAc/heptane to give title compound as colorless oil (451 mg, 44%). ^{1}H NMR (400MHz, $CDCl_3$) δ 3.64 - 3.55 (m, 1H), 3.50 (m, 2H), 3.43 - 3.32 (m, 2H), 3.29 (s, 3H), 3.27 - 3.19 (m, 1H), 3.17 - 3.00 (m, 2H), 2.32 - 2.18 (m, 1H), 2.16 - 2.04 (m, 1H), 1.41 (s, 9H), 0.84 (s, 9H), 0.00 (s, 6H).

Step 2: Synthesis of *tert*-butyl (3*S*,4*S*)-3-(hydroxymethyl)-4-(methoxymethyl)pyrrolidine-1-carboxylate

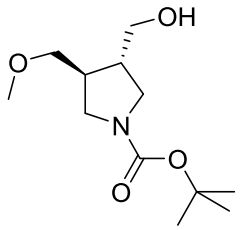

TBAF (1.0M in THF, 2.45 mL, 2.45 mmol) was added to a solution of *tert*-butyl (3S, 4S)-3-(((*tert*-butyldimethylsilyl)oxy)methyl)-4-(methoxymethyl)pyrrolidine-1-carboxylate (290 mg, 0.81 mmol) in THF (5 mL). The mixture was stirred at RT for 1h. The reaction was quenched with H_2O (30 mL) and extracted with EtOAc (2x30 mL). The combined organic layers were dried over $MgSO_4$ and concentrated. The crude product was used in next step.

Preparation of *tert*-butyl (3,4-trans)-3-fluoro-4-(hydroxymethyl)pyrrolidine-1-carboxylate

Step 1: Preparation of (1Z)-3-ethoxy-3-oxoprop-1-en-1-yl benzoate

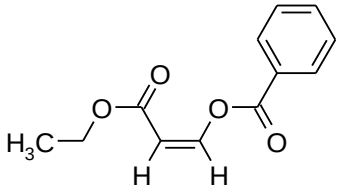

To a suspension of benzoic acid (24.4 g, 200 mmol), silver hexafluorophosphate(V) (253 mg, 1 mmol), chlorotriphenylphosphine gold(I) (495 mg, 1 mmol) in toluene (125 mL) was added ethyl prop-2-ynoate (5.1 mL, 50 mmol). The reaction mixture was stirred and heated at 60 °C for 16 h. The volatiles were removed to give a residue, which was dissolved in ethyl acetate (200 mL) with some trace insoluble material being removed by filtration. The filtrate was washed with saturated aqueous $NaHCO_3$ (with gas evolved - CAUTION) until there was no further gas evolution, and evaporated to give a light brown oil. This oil was purified *via* flash chromatography (eluting with a gradient of 0 – 100 % EtOAc in heptanes) to give the title compound (10.96 g, 99 %) as a colorless oil, which solidified to afford needle-liked crystals. ^{1}H NMR (400 MHz, $CDCl_3$) δ 8.24 - 8.32 (m, 2 H) 7.85 (d, *J* = 7.09 Hz, 1 H) 7.63 - 7.72 (m, 1 H) 7.48 - 7.58 (m, 2 H) 5.44 (d, *J* = 7.21 Hz, 1 H) 4.29 (q, *J* = 7.21 Hz, 2 H) 1.38 (t, *J* = 7.15 Hz, 3

H). ^{13}C NMR (101 MHz, $CDCl_3$) δ 164.15, 162.55, 144.54, 134.31, 130.66, 128.74, 127.90, 103.38, 60.30, 14.28.

Step 2: Preparation of ethyl (3,4-cis)-4-(benzoyloxy)-1-benzylpyrrolidine-3-carboxylate

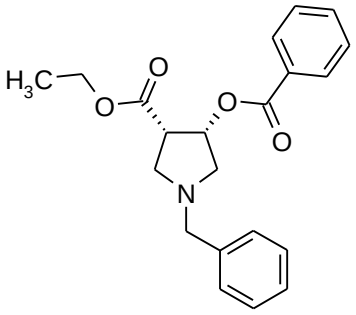

A solution of (1*Z*)-3-ethoxy-3-oxoprop-1-en-1-yl benzoate (6.6 g, 30 mmol) in 2-MeTHF (80 mL) was cooled to 0 °C in a water/ice bath and TFA (605 µL, 6 mmol) was added. A solution of *N*-benzyl-1-methoxy-*N*-[(trimethylsilyl)methyl]methanamine (11.5 mL, 45 mmol) in 2-MeTHF (20 mL) was added dropwise and the resulting solution was stirred at ambient temperature for 20 h. The reaction was diluted with ethyl acetate (100 mL) and saturated aqueous $NaHCO_3$ (30 mL). The organic layer was separated, dried over Na_2SO_4 and evaporated to give a light yellow oil, which was purified *via* flash chromatography (eluting with a gradient of 0 – 100 % EtOAc in heptanes) to give the title compound (10.48 g, 99 %) as a colorless oil. LC-MS (APCI) *m/z* for $C_{21}H_{23}NO_4$ 354.2 $(M+H)^+$; ^1H NMR (400 MHz, $CDCl_3$) δ 7.95 - 8.03 (m, 2 H) 7.53 - 7.61 (m, 1 H) 7.41 - 7.48 (m, 2 H) 7.28 - 7.38 (m, 5 H) 7.21 - 7.27 (m, 1 H) 5.72 (ddd, *J* = 7.58, 5.87, 3.91 Hz, 1 H) 3.97 - 4.17 (m, 2 H) 3.73 (d, *J* = 3.30 Hz, 2 H) 3.32 - 3.47 (m, 2 H) 3.01 - 3.17 (m, 2 H) 2.62 (dd, *J* = 10.88, 3.91 Hz, 1 H) 1.09 (t, *J* = 7.15 Hz, 3 H).

Step 3: Preparation of 1-*tert*-butyl 3-ethyl (3,4-cis)-4-(benzoyloxy)pyrrolidine-1,3-dicarboxylate

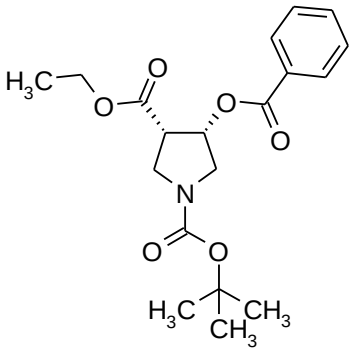

A solution of ethyl (3,4-cis)-4-(benzoyloxy)-1-benzylpyrrolidine-3-carboxylate (7.78 g, 22 mmol) in ethyl acetate (200 mL) was degassed with nitrogen and di-*tert*-butyl dicarbonate (5.3 g, 24 mmol), $Pd(OH)_2$ (20 wt % on carbon, 1 g) were added. The resulting reaction mixture was stirred under hydrogen atmosphere (balloon) for 20 h. The catalyst was removed by filtration, and the filtrate was evaporated to give a colorless oil. This oil was purified *via* flash chromatography (eluting with a gradient of 0 – 100 % EtOAc in heptanes) to give the title compound as a colorless oil, which solidified to a white solid (6.85 g, 86 %). LC-MS (APCI) *m/z* for $C_{19}H_{25}NO_6$ 264.2 $(M+H)^+$; ^{1}H NMR (400 MHz, $CDCl_3$) δ 7.98 (d, *J* = 7.34 Hz, 2 H) 7.53 - 7.62 (m, 1 H) 7.38 - 7.50 (m, 2 H) 5.76 (br. s., 1 H) 4.00 - 4.23 (m, 2 H) 3.57 - 3.99 (m, 4 H) 3.35 (br. s., 1 H) 1.47 (d, *J* = 10.15 Hz, 9 H) 1.13 (t, *J* = 7.09 Hz, 3 H). The *cis*-configuration of the title compound was confirmed by small molecule X-ray crystallography

Step 4: Preparation of *tert*-butyl (3,4-cis)-3-hydroxy-4-(hydroxymethyl)pyrrolidine-1-carboxylate

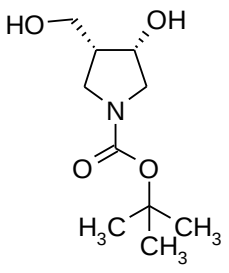

A solution of 1-*tert*-butyl 3-ethyl (3,4-cis)-4-(benzoyloxy)pyrrolidine-1,3-dicarboxylate (3.5 g, 9.6 mmol) in THF (60 mL) was cooled in an ice/water bath under nitrogen atmosphere and borane dimethylsulfide (3.7 mL, 39 mmol) was added. The resulting reaction solution was stirred and heated at 50 °C (oil bath temperature) for 20 h. The reaction was then cooled in a water/ice bath and was carefully quenched with methanol (couple drops at first, 20 mL total) under nitrogen atmosphere. The volatiles were removed to give a colorless residue, which was purified *via* flash chromatography (eluting with a gradient of 0 – 100 % EtOAc in heptanes) to give the title compound as a colorless oil (1.88 g, 90 %) which solidified on standing to a white solid. LC-MS (APCI) *m/z* for $C_{10}H_{19}NO_4$ 118.2 $(M+H)^+$; ^{1}H NMR (400 MHz, $CDCl_3$) δ 4.48 (d, *J* =2.57 Hz, 1 H) 3.90 (br. s., 2 H) 3.40 - 3.56 (m, 3 H) 3.30 - 3.40 (m, 1 H) 3.14 - 3.27 (m, 1 H) 2.73 - 2.99 (m, 1 H) 2.34 (br. s., 1 H) 1.46 (s, 9 H).

Step 5: Preparation of *tert*-butyl (3,4-cis)-3-[(acetyloxy)methyl]-4-hydroxypyrrolidine-1-carboxylate

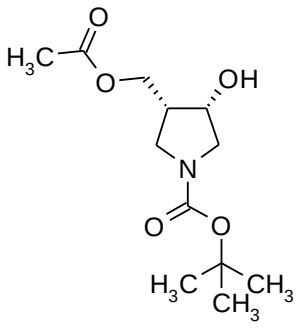

A solution of *tert*-butyl (3,4-cis)-3-hydroxy-4-(hydroxymethyl)pyrrolidine-1-carboxylate (1.4 g, 6.4 mmol) in THF (30 mL) was cooled in an ice/water bath and 2,6-lutidine (1.50 mL, 13 mmol) was added. Acetyl chloride (0.47 mL, 6.4 mmol) was added slowly over a few minutes. The reaction mixture turned cloudy and was stirred in a cold (ice-water?) bath and allowed to warm

to ambient temperature over 1 h. More 2,6-lutidine (1.5 mL, 13 mmol) and acetyl chloride (0.47 mL, 6.4 mmol) were added while cooling in ice/water bath. Stirring at ambient temperature continued for another 2 h. The reaction was cooled in a water bath, was quenched with water (2 mL) and brine (5 mL) and diluted with ethyl acetate (30 mL). The organic layer was separated, dried over Na_2SO_4 and evaporated to give a colorless oil, which was purified *via* flash chromatography (eluting with a gradient of 0 – 100 % EtOAc in heptanes) to give the title compound (1.64 g, 98 %) as a colorless oil. LC-MS (APCI) *m/z* for $C_{12}H_{21}NO_5$ 160.1 $(M+H)^+$; ^{1}H NMR (400 MHz, $CDCl_3$) δ 4.48 (q, *J* = 11.33 Hz, 1 H) 4.24 (d, *J* = 11.37 Hz, 1 H) 4.04 (d, *J* = 11.13 Hz, 1 H) 3.41 - 3.65 (m, 3 H) 3.15 (t, *J* = 10.76 Hz, 1 H) 2.53 (s, 1 H) 2.41 (br. s., 1 H) 2.11 (s, 4 H) 1.46 (s, 9 H).

Step 6: Preparation of *tert*-butyl (3,4-trans)-3-[(acetyloxy)methyl]-4-fluoropyrrolidine-1-carboxylate

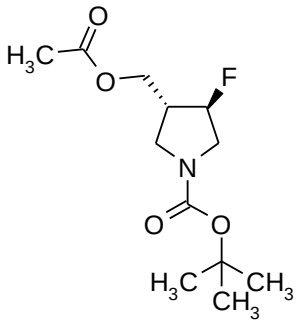

To a solution of *tert*-butyl (3,4-cis)-3-[(acetyloxy)methyl]-4-hydroxypyrrolidine-1-carboxylate (1.20 g, 4.6 mmol) in CH_2Cl_2 (30 mL) under a nitrogen atmosphere at 0 °C was added Deoxo-Fluor™ (1.29 mL, 6.9 mmol). The mixture was stirred at 0 °C for 1 h. More Deoxo-Fluor™ (0.7 mL) was added and stirring was continued for another 15 min. The reaction was carefully quenched with saturated aqueous $NaHCO_3$ (5 mL). The organic layer was separated, dried over

Na_2SO_4 and evaporated to give a residue, which was purified *via* flash chromatography (eluting with a gradient of 0 – 100 % EtOAc in heptanes) to give a colorless oil (718 mg). NMR and LCMS showed a mixture of the title compound and *tert*-butyl 3-[(acetyloxy)methyl]-2,5-dihydro-1*H*-pyrrole-1-carboxylate product at about 6:4 ratio. This material was used crude in the next step.

Step 7: Preparation of *tert*-butyl (3,4-trans)-3-fluoro-4-(hydroxymethyl)pyrrolidine-1-carboxylate

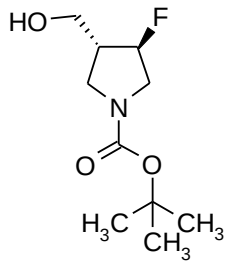

To a crude solution of *tert*-butyl (3,4-trans)-3-[(acetyloxy)methyl]-4-fluoropyrrolidine-1-carboxylate (crude 4.5 mmol ca.) in THF (10 mL) was added water (5 mL) and solid LiOH (269 mg, 11.2 mmol). The reaction mixture was stirred at ambient temperature for 2 h and the reaction was diluted with ethyl ether (20 mL). The organic layer was separated, dried over Na_2SO_4 and evaporated to give a colorless oil. LCMS and NMR indicated a mixture of the title compound and *tert*-butyl 3-(hydroxymethyl)-2,5-dihydro-1*H*-pyrrole-1-carboxylate at about 6:4 ratio. This was used as is in subsequent steps

Preparation of *tert*-butyl (3*R*,4*R*)-3-((tert-butyldimethylsilyl)oxy)-4-(hydroxymethyl)pyrrolidine-1-carboxylate

Step 1: Synthesis of *tert*-butyl (3*R*,4*R*)-3-((*tert*-butyldimethylsilyl)oxy)-4-((trityloxy)methyl)-pyrrolidine-1-carboxylate

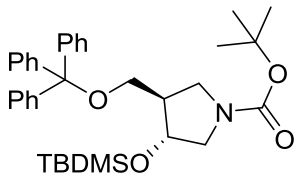

(3*R*,4*R*)-3-((*tert*-butyldimethylsilyl)oxy)-1-((*S*)-1-phenylethyl)-4-((trityloxy)methyl)pyrrolidine (343.0 mg, 0.594 mmol) was dissolved in 20 mL of ethanol (0.03 M). Di-*t*-butyl-dicarbonate (175.6 mg, 0.805 mmol) and palladium hydroxide on carbon (75 mg, 20% Pd, wet) were added to this solution. The resultant mixture was degassed by evacuation until solvent began to boil, followed by argon fill (3 cycles) then evacuated and filled with hydrogen from a balloon (3 cycles). The mixture was stirred under hydrogen balloon for 19 h and filtered through Celite® to remove catalyst. The filter cake was rinsed several times with methanol and the combined filtrates were concentrated. The residue was dissolved in methanol and purified by silica gel column chromatography eluting with 0-30% ethyl acetate in heptane to yield the title product (314 mg, 92% yield). ^{1}H NMR (400 MHz, DMSO-d_6) δ 7.22 - 7.39 (m, 15 H), 4.06 - 4.14 (m, *J* = 5.68, 5.68 Hz, 1 H), 3.43 - 3.55 (m, 1 H), 3.26 (d, *J* = 5.31 Hz, 1 H), 2.89 - 3.14 (m, 4 H), 2.20-2.29 (m, *J* = 5.31 Hz, 1 H), 1.38 (s, 9 H), 0.78 (d, *J* = 2.78 Hz, 9 H), -0.02 (s, 3 H), -0.07 (d, *J* = 7.58 Hz, 3 H).

Step 2: Synthesis of *tert*-butyl (3*R*,4*R*)-3-((*tert*-butyldimethylsilyl)oxy)-4-(hydroxymethyl)pyrrolidine-1-carboxylate

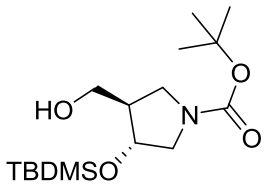

tert-Butyl-(3*R*,4*R*)-3-((*tert*-butyldimethylsilyl)oxy)-4-((trityloxy)methyl)pyrrolidine-1-carboxylate (1.67 g, 2.91 mmol) was dissolved in 30 mL of 1% w/v iodine/methanol solution. The resultant solution was stirred at 50 °C for 90 h. After concentration of the solvent, the residue was diluted with 50 mL of ethyl acetate and washed with 20 mL of sat. aq. sodium thiosulfate. The organic layer was washed again with 20 mL of deionized water, dried over magnesium sulfate and filtered. The filtrate was concentrated and purified by silica gel column chromatography eluting with 0-20% of ethyl acetate in heptane to give the title compound (438 mg, 45% yield). LC-MS(APCI) *m/z* for product minus Boc group 232.2 $(M+H)^+$; ^{1}H NMR (400 MHz, $CDCl_3$) δ 4.17 (br. s., 1 H), 3.52 - 3.76 (m, 4 H), 3.15 (dd, *J* = 10.74, 5.68 Hz, 2 H), 2.28 (d, *J* = 6.06 Hz, 1 H), 1.41 - 1.51 (m, 9 H), 0.89 (s, 9 H), 0.09 (s, 3 H), 0.08 (s, 3 H).

ADDITIONAL DATA ON PROTEOME-WIDE SELECTIVITY.

Figure SI-1. (A) In situ labeling profiles of P_**22** (Probe_**22**, left) and P_**23** (Probe_**23**, right) for one hour in H1975 cells in triplicate analysis and separated into particulate (left) and soluble (right) proteomes. (B) A comparison graphical analysis of in situ reactivity profile for P_**22** and P_**23** based on full gel lane band intensity (with that of EGFR and similar molecular weight proteins subtracted). Intensity from P_**22** is defined as 100% and the intensity of P_**23** is presented as a percentage of P_**22**. (C) Time course in situ labeling profiles of 1 µM Probe_**22** (left) and Probe_**23** (right) in H3255 cells separated into soluble (top) and particulate (bottom) proteomes. H3255 cells were treated for 15 minutes to 24 hours before being harvested. Lysates were analyzed by gel-based florescence and gels are shown in grayscale.

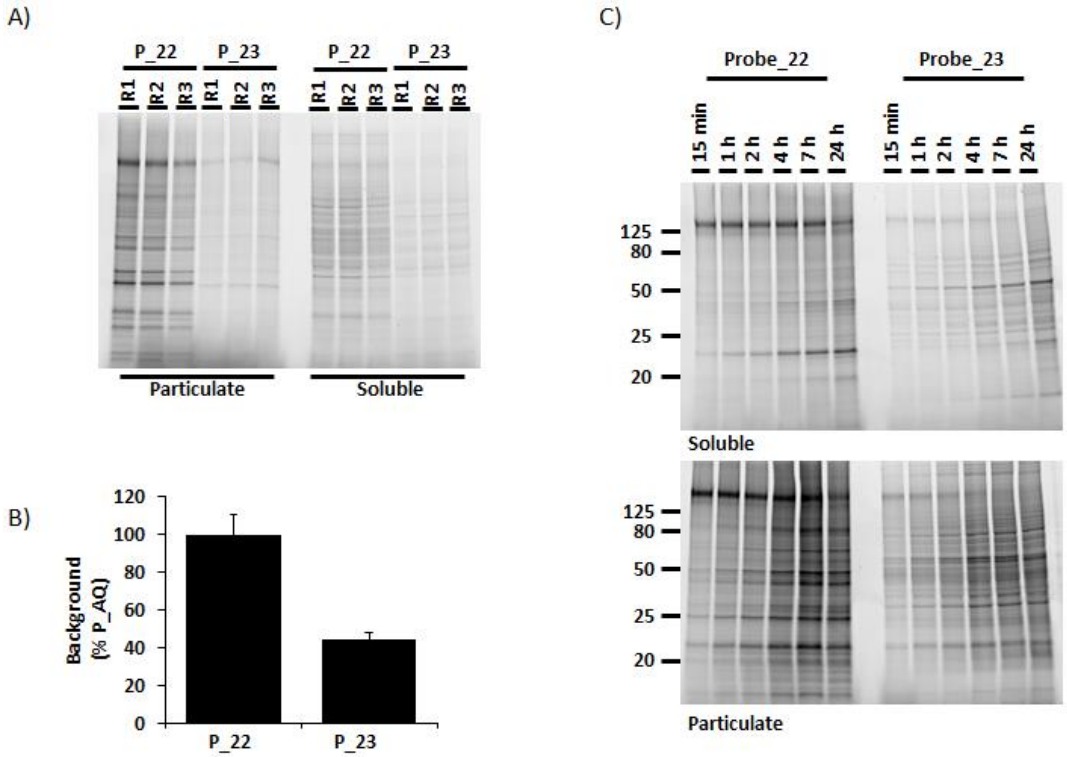

KINASE SELECTIVITY DATA FOR COMPOUND 1.

Kinome selectivity of **1** was explored against a panel of 267 human kinases using a mobility shift assay format at Carna Biosciences. At 1 μM concentration of **1**, for kinases without a cysteine residue corresponding to EGFR-Cys797, 92 kinases had >50% inhibition and 32 kinases had >90% inhibition. Using a higher, more cell-like concentration of adenosine triphosphate (ATP) (1 mM), 20 of 54 kinases tested exhibited >50% inhibition by 1000 nM of **1**. Of the 10 protein kinases with a similarly positioned cysteine residue, 7 of them were inhibited >90% by 100 nM of **1**.

Between reversible inhibition mechanism and irreversible inhibition mechanism, translation from enzyme activity to cellular functional activity could be very different; therefore,

evaluating kinase selectivity in cellular functional assays may better reflect the kinase selectivity for irreversible kinase inhibitors. Consequently, **1** was tested against 14 non-target kinases in 13 cellular assays, with JAK1/3 activities measured in one assay. These 14 non-target kinases were selected by meeting the following two criteria, over 75% enzymatic inhibition at 1 μM and the availability of the corresponding cellular assays. Compound **1** is at least 25-fold less potent against the non-target kinases which were tested, with the exception of JAK1/3 (5-fold less potent), in relation to its target potency on EGFR double mutant Del/T790M.

Table SI-3. Broad kinase selectivity analysis of compound 1 (mobility shift assay)

% Inhibition PF-06459988-00 (1 μM)												
ABL	35	LCK	61	CaMK4	-6	HIPK4	44	MST2	69	PKCζ	-4
ACK	40	LTK	80	CDC2/CycB1	83	IKKα	-1	MST3	18	PKCη	3
ALK	76	LYNa	40	CDC7/ASK	-7	IKKβ	-1	MST4	9	PKCθ	9
ARG	24	LYNb	35	CDK2/CycA2	97	IKKε	25	NDR1	53	PKCι	-4
AXL	100	MER	93	CDK2/CycE1	96	IRAK1	43	NDR2	55	PKD1	73
BRK	16	MET	54	CDK3/CycE1	81	IRAK4	20	NEK1	19	PKD2	74
CSK	5	MUSK	100	CDK4/CycD3	53	JNK1	50	NEK2	5	PKD3	64
DDR1	67	PDGFRα	94	CDK5/p25	94	JNK2	64	NEK4	22	PKN1	36
DDR2	58	PDGFRβ	90	CDK6/CycD3	28	JNK3	78	NEK6	-1	PKR	51
EPHA1	26	PYK2	100	CDK7/CycH/MAT1	81	LATS2	22	NEK7	-1	PLK1	10
EPHA2	4	RET	104	CDK9/CycT1	53	LOK	43	NEK9	34	PLK2	8
EPHA3	2	RON	28	CGK2	21	MAP2K1_Cascade	8	NuaK1	98	PLK3	8
EPHA4	10	ROS	78	CHK1	15	MAP2K2_Cascade	4	NuaK2	93	PRKX	0
EPHA5	14	SRC	49	CHK2	46	MAP2K3_Cascade	8	p38α	5	QIK	56
EPHA6	43	SRM	-5	CK1α	7	MAP2K4_Cascade	-20	p38β	-2	RAF1_Cascade	12
EPHA7	35	SYK	91	CK1γ1	42	MAP2K5_Cascade	33	p38γ	10	ROCK1	27
EPHA8	9	TEC	96	CK1γ2	60	MAP2K6_Cascade	3	p38δ	33	ROCK2	44
EPHB1	21	TIE2	35	CK1γ3	50	MAP3K1_Cascade	-21	p70S6K	73	RSK1	59
EPHB2	4	TNK1	92	CK1δ	28	MAP3K2_Cascade	51	p70S6Kβ	14	RSK2	60
EPHB3	-10	TRKA	101	CK1ε	7	MAP3K3_Cascade	38	PAK1	0	RSK3	86
EPHB4	-2	TRKB	102	CK2α1/β	9	MAP3K4_Cascade	3	PAK2	16	RSK4	65
FAK	53	TRKC	103	CK2α2/β	32	MAP3K5_Cascade	10	PAK4	68	SGK	12
FER	88	TXK	101	CLK1	95	MAP4K2	85	PAK5	46	SGK2	3
FES	42	TYK2	94	CLK2	79	MAPKAPK2	-8	PAK6	34	SGK3	-5
FGFR1	85	TYRO3	60	CLK3	25	MAPKAPK3	-2	PASK	-3	SIK	33
FGFR2	93	YES	86	COT_Cascade	1	MAPKAPK5	-4	PBK	-7	skMLCK	3
FGFR3	92	ZAP70	52	CRIK	14	MARK1	66	PDHK2	-5	SLK	51
FGFR4	53	AKT1	0	DAPK1	49	MARK2	67	PDHK4	-2	SRPK1	7
FGR	45	AKT2	-2	DCAMKL2	3	MARK3	73	PDK1	40	SRPK2	4
FLT1	98	AKT3	0	DLK_Cascade	32	MARK4	82	PEK	34	TAK1-TAB1_Cascade	36
FLT3	103	AMPKα1/β1/γ1	27	DYRK1A	32	MELK	66	PGK	2	TAOK2	29
FLT4	102	AMPKα2/β1/γ1	46	DYRK1B	30	MGC42105	0	PHKG1	37	TBK1	53
FMS	72	AurA	99	DYRK2	37	MINK	33	PHKG2	6	TNIK	73
FRK	11	AurA/TPX2	97	DYRK3	6	MLK1_Cascade	46	PIM1	-2	TSSK1	90
FYN	63	AurB	96	EEF2K	-3	MLK2_Cascade	19	PIM2	0	TSSK2	10
HCK	32	AurC	91	Erk1	10	MLK3_Cascade	40	PIM3	7	TSSK3	-3
HER4	99	BRAF_Cascade	12	Erk2	10	MNK1	1	PKACα	8	WNK1	-3
IGF1R	28	BRSK1	14	Erk5	14	MNK2	11	PKACβ	-2	WNK2	-3
INSR	62	BRSK2	18	GSK3α	76	MOS_Cascade	-3	PKACγ	7	WNK3	-7
IRR	38	CaMK1α	1	GSK3β	71	MRCKα	-3	PKCα	9	PIK3CA/PIK3R1	4
ITK	104	CaMK1δ	4	Haspin	3	MRCKβ	28	PKCβ1	19	SPHK1	0
JAK1	84	CaMK2α	-1	HGK	78	MSK1	12	PKCβ2	18	SPHK2	-4
JAK2	99	CaMK2β	-2	HIPK1	42	MSK2	1	PKCγ	20		
KDR	95	CaMK2γ	4	HIPK2	36	MSSK1	3	PKCδ	23		
KIT	79	CaMK2δ	10	HIPK3	51	MST1	92	PKCε	-1		

At 1000 nM in the Carna Biosciences mobility shift kinase assay, using a 267-kinase panel. 247 human kinases analyzed at a Km concentration of ATP and 20 kinases were tested in a cascade assay (as specified) with 1 mM ATP.

Table SI-4. Selectivity of compound 1 at 1 µM and 1 mM ATP in the Carna Biosciences mobility shift kinase assay. 54 human kinases analyzed.

% Inhibition @ 1 mM ATP and 1 µM PF-06459988							
ALK	21.3	FAK	6.7	JAK1	42.3	ROS	29.2
AurB	58.5	FER	25.0	JAK2	77.7	RSK1	-13.0
AurC	48.5	FGFR3	67.4	JNK1	11.1	SYK	40.8
BLK	87.8	FGFR4	41.2	JNK2	10.3	TEC	85.2
BMX	98.0	FLT1	85.6	KIT	68.5	TNK1	65.7
CDC2/CycB1	32.5	FLT3	101.2	LTK	42.3	TRKB	98.2
CDK2/CycA2	71.8	FLT4	99.6	MST1	50.7	TSSK1	13.4
CDK2/CycE1	83.8	FMS	42.5	MUSK	46.5	TXK	89.5
CDK4/CycD3	26.0	FYN	8.9	P70S6K	36.8	TYK2	54.9
CDK5/p25	34.9	GSK3α	4.5	PDGFRα	42.8	TyrO3	29.5
CDK7/CycH/MAT1	26.6	HER2	-10.8	PDGFRβ	24.4	YES	27.7
CDK9/CycT1	2.1	HER4	34.2	PDK2	-2.9	ZAP70	0.7
DDR1	32.5	HGK	-5.3	PYK2	97.0		
DDR2	14.2	ITK	99.6	RET	59.7		

Table SI-5. Compound 1 Selectivity to Protein Kinases with Reactive Cysteine Residues in the Hinge Region of the Catalytic Domain (Similar to EGFR-Cys$_{797}$)

Kinase	**Percent Inhibition at 100 nM**
EGFR-WT	15
HER2	17
JAK3	103
HER4	8
BLK	94
TXK	98
BTK	102
TEC	84
BMX	103
ITK	77
MAP2K7	2

Inhibition was evaluated using a mobility shift kinase assay at Carna Bioscience. Reactions were conducted using a K_m concentration of ATP, except MAP2K7 was tested in a cascade assay with 1 mM ATP.

Table SI-6. Cellular Potency of compound 1 on Inhibition of Non-target Kinases[a]

Kinase	Cell IC50 nM (n)	Fold Selectivity[b]
BTK	9000 (n=1)	643
JAK3	76 (n=1)	5
AUR-A	496 (n=3)	35
AUR-B	400 (n=1)	29
AXL	>10,000 (n=2)	714
FGFR1	688 (n=1)	49
FGFR2	521 (n=1)	37
MER	>10,000 (n=1)	714
ALK	7135 (n=1)	510
TRKA	4127 (n=5)	295
TRKB	1041(n=3)	74
FLT3	343 (n=1)	25
PDGFRβ	13000 (n=1)	929
JAK1	76 (n=1)	5

[a]These 14 non-target kinases were selected by meeting the following two criteria, over 75% enzymatic inhibition at 1 μM and the availability of the corresponding cellular assays. Cellular phosphorylation assays for AXL, FGFR1/2, MER, ALK, TRKA/B, FLT3, JAK1/3, and BTK were performed at Pfizer. The Aurora A assay was conducted at Caliper Life Science (Waltham, MA, USA), and the Airora B and platelet-derived growth factor receptorβ (PDGFRβ) assays at ProQinase (Freiburg, Germany).

[b]Fold selectivity is based on values of non-target kinase cellular IC_{50} over pEGFR IC_{50} in PC9-DRH, the least sensitive NSCLC model among the EGFR double mutant targets models.

LIGAND TORSIONAL STRAIN ENERGY ANALYSIS FOR 15 AND 16.

The torsional strain energy profile for the bond between 6-PP and the ether oxygen is calculated for both 5-H PP derivative (**15**) and 5-Cl PP derivative (**16**). The four atoms selected for torsional profile calculation are highlighted in Scheme 1. Amber force field was used for the calculation. As is illustrated in Figure SI-2, the torsional energy is the highest at 180 degrees for both **15** and **16**, and the torsional energy is 5.6 kcal/mol for **15**, and is 12.5 for **16**. This indicates introduction of 5-Cl significantly restricts the rotatability of the bond between 6-PP and the ether oxygen, hence restricting the conformation of the linker.

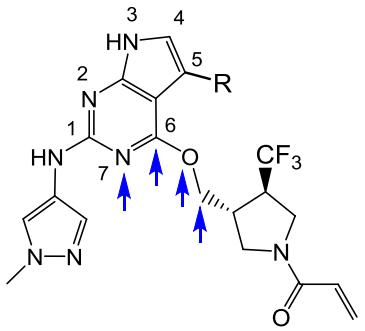

15: R = H
16: R = Cl

Figure SI-2A. Structures for **15** and **16**. Highlighted atoms were used to calculate torsional energy profile.

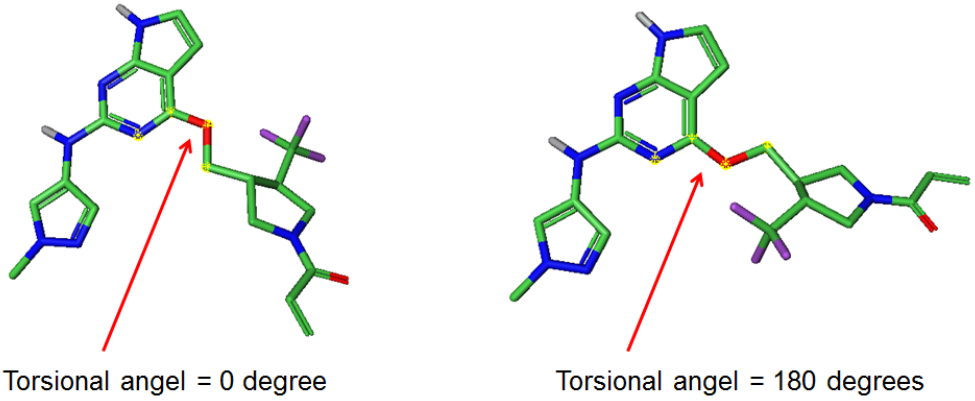

Figure SI-2B. Conformations for **15** when the torsional angle is 0 degree and 180 degrees, respectively.

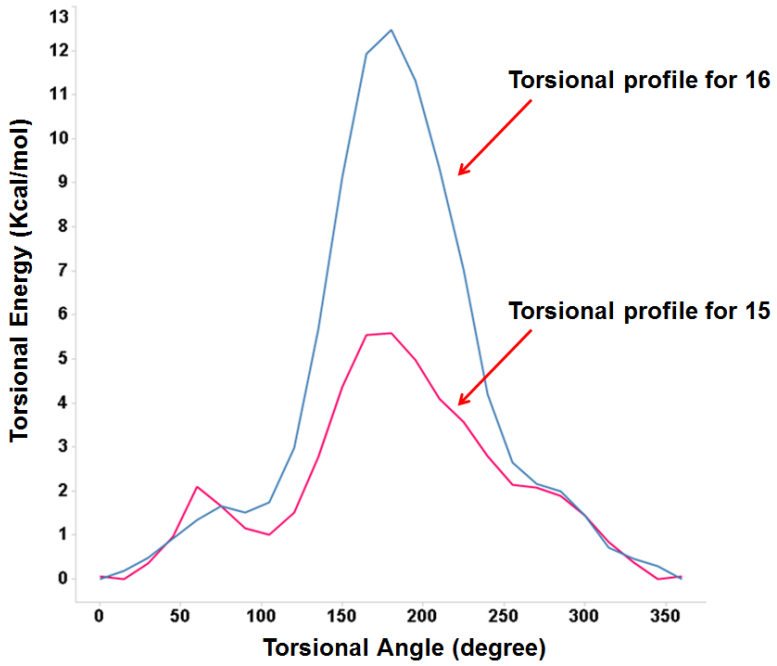

Figure SI-3. Comparison of torsional energy profiles for **15** and **16**.

LIGAND STRAIN ENERGY ANALYSIS FOR BOUND CONFORMATION OF COMPOUND 1 IN EGFR DM.

Shown below is the bound conformation of Compound **1** in EGFR DM. Ligand strain energy analysis was carried out using Bachmin V2.0[2] with 4 different force fields. The results are summarized in Table SI-7 below, indicating low strain energy is associated with the bound conformation of **1**.[2]

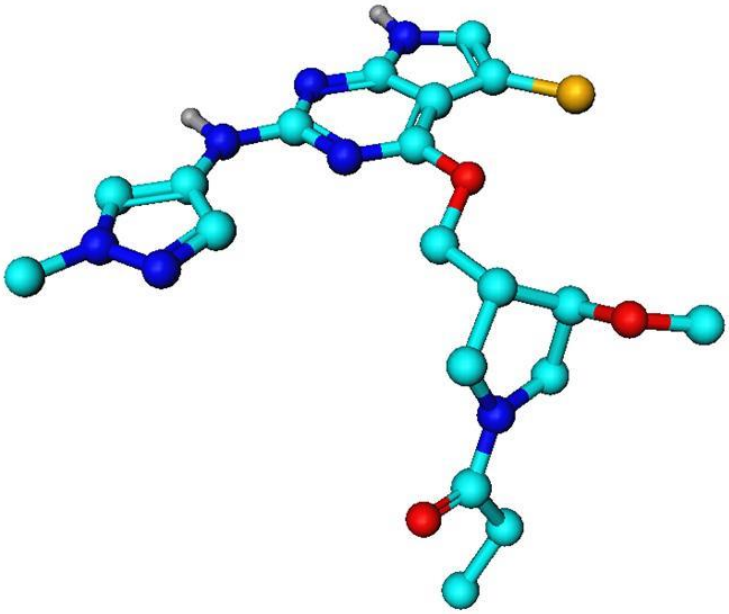

Figure SI-4. Bound conformation of **1** in complex with monomeric L858R/T790M EGFR cocrystal structure.

Table SI-7. Ligand Conformational Strain Energy Calculated Using Bachmin V2.0.

Strain Type	Amber (kcal/mol)	OPLSA (kcal/mol)	MMFF94 (kcal/mol)	OPLS2005 (kcal/mol)	MeanStrain (kcal/mol)	StdDevStrain (kcal/mol)
Local	1.06067	1.12118	0.941922	1.06692	1.04762	0.0755441
Global	1.52232	2.3844	1.42526	5.77177	2.77594	2.04322

MODELING OF COMPOUND 10 IN WT EGFR PROTEIN. 2.9 Å proximity of PP core to the gatekeeper Thr790 provides selectivity against EGFR WT due to electrostatic clash. Experiments so far suggest that the DM samples a larger conformational space than does the

WT; DM also has altered conformational energy landscape.[3] So it is more likely that WT enzyme has a much greater energy barrier to adopt the specific conformation recognized by the ligand than does the DM, and it is manifested in the selectivity profile.

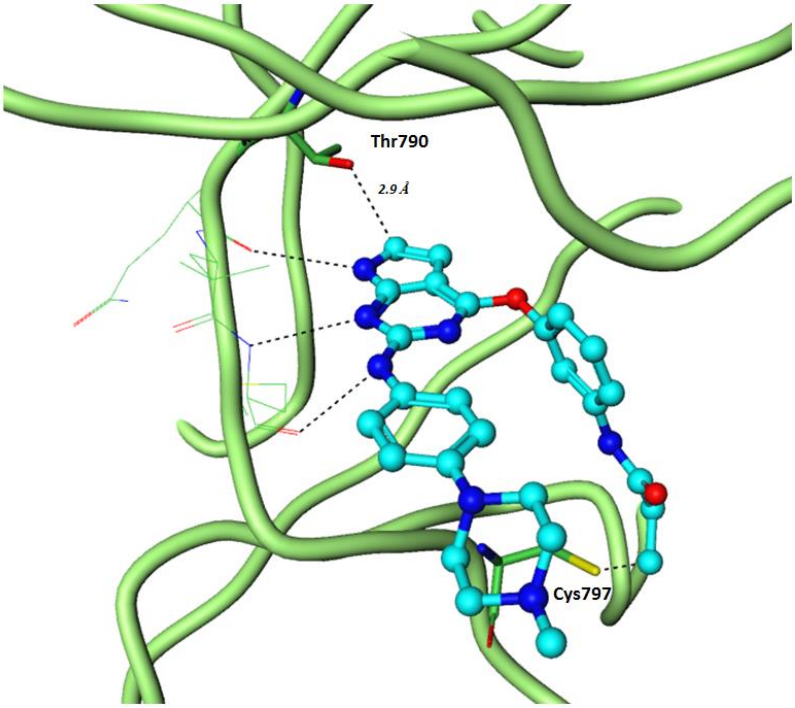

Figure SI-5. Modeling of compound **10** in WT EGFR protein.

SUMMARY OF BIOCHEMICAL AND CELLULAR POTENCY FOR COMPOUND 1 WITH SMILES STRING

Table SI-8. Summary Table with SMILES String for Compound 1.

SMILES string for compound **1**	Cn1cc(cn1)Nc2nc3c(c(c[nH]3)Cl)c(n2)OC[C@H]4CN(C[C@@H]4OC)C(=O)C=C	
*K*i (nM)	L858R/T790M	13
k_{inact} (s^{-1})		0.02
k_{inact}/K_i ($M^{-1}s^{-1}$)		1,530,000
Ki^{est} (nM)	WT	1,600
k_{inact}/K_i^{est} ($M^{-1}s^{-1}$)		4,520
H1975 IC_{50} (nM)	L858R/T790M	13
PC9-DRH IC_{50} (nM)	Del/T790M	7
H3255 IC_{50} (nM)	L858R	21
PC9 IC_{50} (nM)	Del	140
A549 IC_{50} (nM)	WT	5,100
Cell IC_{50} Ratio (A549/H1975)	WT/L858R_T790M	392

REFERENCES.

1. Schwartz, P. A.; Kuzmic, P.; Solowiej, J.; Bergqvist, S.; Bolanos, B.; Almaden, C.; Nagata, A.; Ryan, K.; Feng, J.; Dalvie, D.; Kath, J. C.; Xu, M.; Wani, R.; Murray, B. W., Covalent EGFR inhibitor analysis reveals importance of reversible interactions to potency and mechanisms of drug resistance. *Proceedings of the National Academy of Sciences of the United States of America* **2014,** *111* (1), 173-8.

2. Perola, E.; Charifson, P. S., Conformational Analysis of Drug-Like Molecules Bound to Proteins: An Extensive Study of Ligand Reorganization upon Binding. *J. Med. Chem.* **2004,** *47* (10), 2499-2510.

3. Gajiwala, K. S.; Feng, J.; Ferre, R.; Ryan, K.; Brodsky, O.; Weinrich, S.; Kath, J. C.; Stewart, A., Insights into the Aberrant Activity of Mutant EGFR Kinase Domain and Drug Recognition. *Structure (Oxford, U. K.)* **2013,** *21* (2), 209-219.